Bio-Design and Manufacturing (2025) 8:672–704
https://doi.org/10.1631/bdm.2400267

REVIEW

Bone implants with triply periodic minimal surface architectures: design, fabrication, and biological performance

Jianhui Li[1] · Haitao Fan[3] · Licheng Hua[1] · Jianke Du[1] · Yong He[2] · Yu'an Jin[1]

Received: 7 July 2024 / Accepted: 7 November 2024 / Published online: 5 July 2025

Abstract

Triply periodic minimal surface (TPMS)-based bone implants are an innovative approach in orthopedic implantology, offering customized solutions for bone defect repair and regeneration. This review comprehensively examines the current research landscape of TPMS-based bone implants, addressing key challenges and proposing future directions. It explores design strategies aimed at optimizing mechanical strength and enhancing biological integration, with a particular emphasis on TPMS structures. These design strategies include graded, hierarchical, and hybrid designs, each contributing to the overall functionality and performance of the implants. This review also highlights state-of-the-art fabrication technologies, particularly advancements in additive manufacturing (AM) techniques for creating metal-based, polymer-based, and ceramic-based bone implants. The ability to precisely control the architecture of TPMS structures using AM techniques is crucial for tailoring the mechanical and biological properties of such implants. Furthermore, this review critically evaluates the biological performance of TPMS implants, focusing on their potential to promote bone ingrowth and regeneration. Key factors, such as mechanical properties, permeability, and biocompatibility, are examined to determine the effectiveness of these implants in clinical applications. By synthesizing existing knowledge and proposing innovative research directions, this review underscores the transformative potential of TPMS-based bone implants in orthopedic surgery. The objective is to improve clinical outcomes and enhance patient care through advanced implant designs and manufacturing techniques.

✉ Yong He
yongqin@zju.edu.cn

✉ Yu'an Jin
jinyuan@nbu.edu.cn

[1] Zhejiang-Italy Joint Lab for Smart Materials and Advanced Structures, School of Mechanical Engineering and Mechanics, Ningbo University, Ningbo 315211, China

[2] State Key Laboratory of Fluid Power and Mechatronic Systems, School of Mechanical Engineering, Zhejiang University, Hangzhou 310058, China

[3] Department of Orthopaedics, The First Affiliated Hospital of Ningbo University, Ningbo 315000, China

Graphical abstract

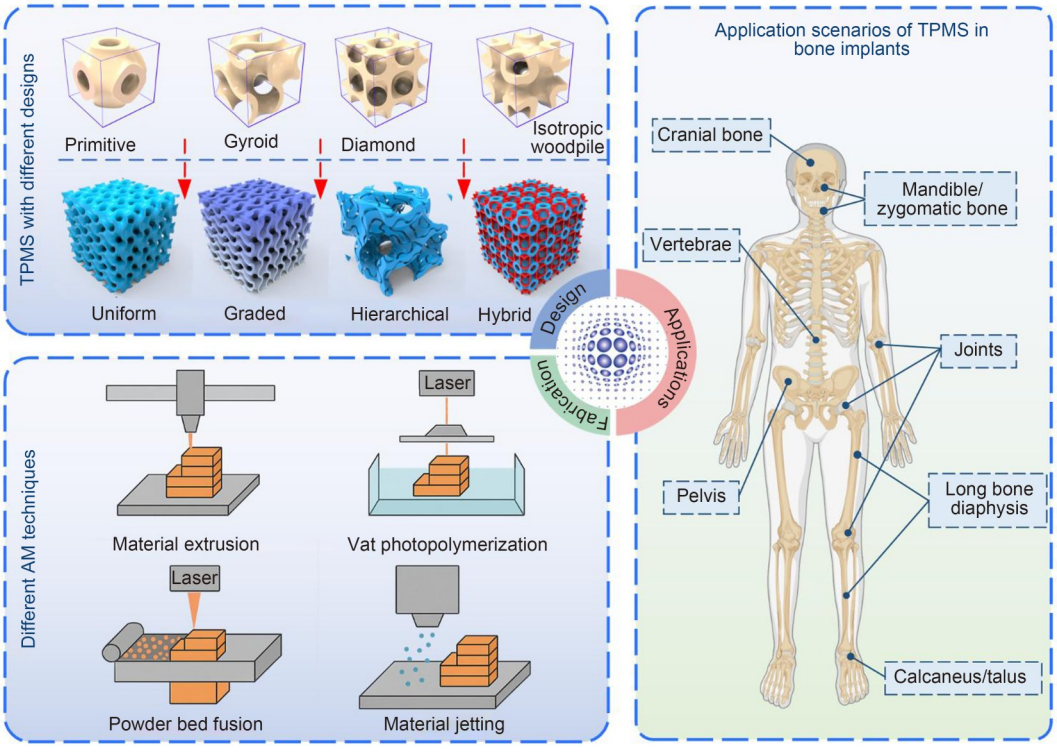

Keywords Triply periodic minimal surface · Bone implants · Design method · Additive manufacturing · Biological performance

1 Introduction

Bone implants play a crucial role in orthopedic and dental surgeries, significantly enhancing the quality of life of patients with bone defects or bone degeneration [1]. These implants replace or support damaged bones, thereby helping restore function and alleviate pain. The design and material properties of these implants are crucial for their success, as they must seamlessly integrate with host tissue while enduring mechanical loads [2]. Traditionally, bone implants have been made from dense, nonporous materials like titanium and its alloys, which are known for their excellent mechanical strength and biocompatibility [3]. However, these dense materials often fail to mimic the intricate, hierarchical structure of natural bone, which is essential for effective osseointegration [4]. This limitation has spurred the development of new approaches that incorporate porous structures to better replicate natural bone environments [5].

One of the most promising advancements in porous bone implants is the use of triply periodic minimal surfaces (TPMSs) [6]. TPMSs are a unique class of mathematical surfaces characterized by their periodicity in three dimensions and their minimal surface area for a given volume. These structures provide high interconnectivity and porosity, which can be precisely controlled through computational design. Examples of TPMS structures include gyroid, Schwarz D, and diamond surfaces, each offering complex geometries that can be tailored to meet specific mechanical and biological requirements [7]. The use of TPMS in bone implants offers several significant advantages. These intricate geometries can be engineered to achieve high strength-to-weight ratios, closely mimicking the mechanical properties of natural bone [8]. This is particularly beneficial for load-bearing applications, where the implant must support physiological loads without failing. Additionally, the interconnected porosity of TPMS structures promotes vascularization and bone ingrowth, which are crucial for the successful integration of the implant with the host bone. This network of interconnected pores facilitates nutrient exchange and waste removal, thus promoting healthy bone tissue development around the implant [9, 10].

The design process is a critical first step in developing effective TPMS-based bone implants, as it directly influences their mechanical and biological performance [11]. This process involves various innovative methods for optimizing the functional properties of implants. Graded design techniques enable the creation of implants with spatially varying properties, mimicking the natural gradation of bone tissue and enhancing the integration between the implant and host bone [12]. Hierarchical design approaches incorporate multiple levels of porosity, from macro to micro scales, to replicate the complex structure of natural bone, thereby improving mechanical stability and biological compatibility [13]. Furthermore, hybrid designs combine different TPMS geometries or integrate TPMS structures with other elements, leveraging the strengths of various configurations to achieve implants with tailored mechanical properties and enhanced functionality [14]. These diverse design methodologies have collectively contributed to the development of advanced TPMS-based bone implants that closely mimic natural bone and meet specific clinical requirements [15].

TPMS-based bone implants are primarily produced using various additive manufacturing (AM) techniques that enable the precise construction of complex geometries inherent to TPMS designs [16]. Laser powder bed fusion (LPBF) is a prominent technique for fabricating metallic implants, particularly with materials such as titanium and its alloys, because of their excellent mechanical properties and biocompatibility [17, 18]. For polymer-based implants, techniques, such as fused deposition modeling (FDM) [19, 20] and stereolithography (SLA) [21, 22] are commonly used. These methods are advantageous for creating lightweight, flexible structures that can be tailored to specific biological and mechanical requirements. Ceramics, which are also known for their outstanding wear resistance and biocompatibility, are often fabricated using extrusion-based AM [23] and digital light processing (DLP) [24, 25]. These techniques enable the creation of intricate TPMS structures that support bone ingrowth and ensure long-term stability in orthopedic applications. The choice of material and manufacturing method is carefully selected based on the specific properties required for the final implant, ensuring that it meets the stringent demands of biomedical applications.

As the field of orthopedic and dental implantology continues to advance, the integration of AM techniques with innovative design principles is crucial for the development of TPMS-based bone implants [26]. The unique geometric properties of TPMS structures, combined with recent progress in computational design and AM, hold significant potential for improving patient outcomes. Despite the rapid growth of research on TPMS structures over the past decade, encompassing numerous studies on design, fabrication, and performance, a comprehensive review specifically focused on TPMS-based bone implants has yet to be published. This review aims to bridge this gap by thoroughly examining the design, fabrication processes, and biological performance of TPMS-based bone implants. Building on this foundation, this review aims to consolidate existing knowledge, identify key challenges, and propose future research directions. The structure of this review, as outlined in Fig. 1, is as follows. Section 2 discusses design strategies. Section 3 summarizes the

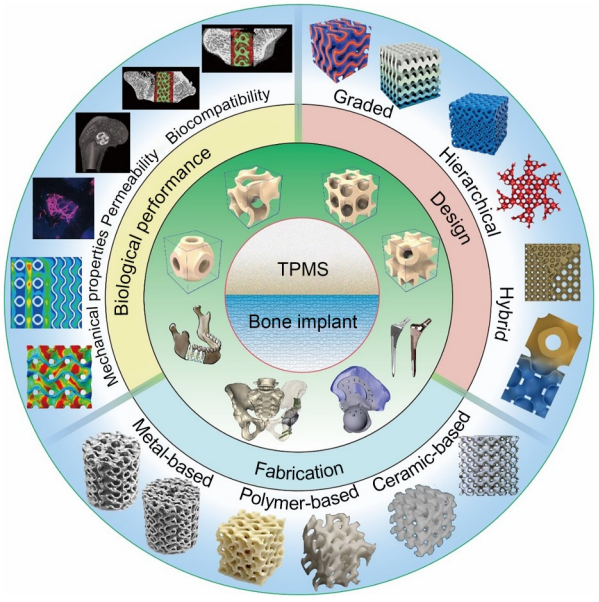

Fig. 1 Overview of TPMS-based bone implants: design, fabrication, and biological performance. Images for "Bone implant" were reproduced from [27] (Copyright 2023, with permission from the authors, licensed under CC BY), [28] (Copyright 2022, with permission from the authors, licensed under CC BY), and [29] (Copyright 2022, with permission from the authors, licensed under CC BY). Images for "Graded" were reproduced from [30] (Copyright 2020, with permission from the authors, licensed under CC BY) and [31] (Copyright 2022, with permission from the authors, licensed under CC BY). Images for "Hierarchical" were reproduced from [32] (Copyright 2020, with permission from the authors, licensed under CC BY) and [33] (Copyright 2021, with permission from the authors, licensed under CC BY-NC-ND). Images for "Hybrid" were reproduced from [34] (Copyright 2020, with permission from John Wiley & Sons, Ltd.) and [35] (Copyright 2022, with permission from the authors, licensed under CC BY-NC-ND). Images for "Ceramic-based" were reproduced from [36] (Copyright 2023, with permission from Elsevier) and [37] (Copyright 2023, with permission from Elsevier). Images for "Polymer-based" were reproduced from [38] (Copyright 2022, with permission from the authors, licensed under CC BY) and [39] (Copyright 2023, with permission from the authors, licensed under CC BY-NC-ND). Images for "Metal-based" were reproduced from [40] (Copyright 2021, with permission from ASM International). Image for "Mechanical properties" was reproduced from [41] (Copyright 2020, with permission from the authors, licensed under CC BY-NC-ND). Image for "Permeability" was reproduced from [42] (Copyright 2024, with permission from Elsevier). lmages for "Biocompatibility" were reproduced from [43] (Copyright 2022, with permission from Elsevier), [44] (Copyright 2023, with permission from Wiley-VCH GmbH), and [45] (Copyright 2022, with permission from the authors, licensed under CC BY)

fabrication methodologies. Section 4 presents the biological performance analysis. Finally, Section 5 presents the conclusions and future prospects.

2 Design of TPMS-based bone implants

The development of TPMS-based bone implants relies heavily on the design process and their biological performance, which are critical for successful clinical applications. Effective design ensures that these implants not only mimic the mechanical properties of natural bone—providing necessary strength and flexibility to withstand physiological loads without causing stress shielding—but also promote optimal biological integration [43]. The key aspects of biological performance include mechanical strength, permeability, and biocompatibility [46–48]. The intricate TPMS structures achieve high permeability, which is essential for nutrient transport, waste removal, and vascularization, facilitating integration with host bone tissue [49, 50]. Biocompatibility is crucial because the materials and surface properties must support cell attachment, proliferation, and differentiation without triggering adverse immune responses [51]. Furthermore, the interconnected porous architecture inherent in TPMS designs promotes bone ingrowth and osseointegration, enhancing long-term stability and functionality [52, 53]. By carefully considering factors such as porosity, pore size, and interconnectivity during the design process, TPMS structures can replicate the hierarchical structure of natural bone, ultimately leading to improved patient outcomes.

2.1 TPMS-based structures

The smooth and continuous surfaces of TPMS minimize stress concentration, thereby improving the mechanical performance and durability under physiological loads. The ability to precisely control the pore size and distribution within TPMS structures allows for the customization of mechanical properties to closely match those of natural bone, thereby reducing the risk of implant failure. Additionally, the inherent geometrical complexity of TPMS can be easily manipulated to facilitate the creation of patient-specific implants with tailored properties to optimize clinical outcomes [54].

Several types of TPMSs, including gyroid, primitive, isotropic woodpile (IWP), and diamond (Fig. 2a), have been used to design bone implants, each characterized by distinct equations and morphologies, as illustrated in Table 1 [55]. These varied morphologies and mathematical formulations allow for the customization of bone implants to meet specific clinical requirements, thereby optimizing mechanical performance and biological compatibility [56].

Moreover, two types of bone scaffolds (Fig. 2c) based on TPMS have been proposed: skeletal and sheet [57]. Skeletal scaffolds are characterized by their framework-like structure, which provides high mechanical strength and rigidity, making them suitable for load-bearing applications. Their open framework facilitates excellent nutrient flow and waste removal, promoting efficient cell migration and bone ingrowth [58]. In contrast, sheet scaffolds feature thin, continuous surfaces that offer a high surface area-to-volume ratio, which is beneficial for cell adhesion and proliferation. The sheet structure can be designed to have varying degrees of flexibility and porosity, allowing for customization based on the specific requirements of the implant site [59]. It has been verified that sheet topologies, particularly sheet diamond, demonstrate 1.3–2.0 times higher peak and plateau stress values than skeletal topologies, while also demonstrating superior toughness [60].

The pore size of TPMS-based bone implants (Fig. 2b) significantly influences their biological and mechanical performance [7]. Optimal pore sizes facilitate cell migration, proliferation, and differentiation, which are crucial for effective osseointegration and bone regeneration [61, 62]. Larger pores enhance nutrient and waste exchange, supporting healthier tissue growth, whereas smaller pores contribute to a higher surface area and mechanical interlocking between the implant and surrounding bone. By adjusting the pore size, TPMS-based implants can be engineered to balance

Table 1 Mathematical equations for different TPMSs

TPMS type	Equation $\boldsymbol{F}(x,y,z)$
Primitive	$\cos\left(\frac{2\pi}{a}x\right)+\cos\left(\frac{2\pi}{b}y\right)+\cos\left(\frac{2\pi}{c}z\right)=n$
Gyroid	$\cos\left(\frac{2\pi}{a}x\right)\sin\left(\frac{2\pi}{b}y\right)+\cos\left(\frac{2\pi}{b}y\right)\sin\left(\frac{2\pi}{c}z\right)+\cos\left(\frac{2\pi}{c}z\right)\sin\left(\frac{2\pi}{a}x\right)=n$
Diamond	$\cos\left(\frac{2\pi}{a}x\right)\cos\left(\frac{2\pi}{b}y\right)\cos\left(\frac{2\pi}{c}z\right)-\sin\left(\frac{2\pi}{a}x\right)\sin\left(\frac{2\pi}{b}y\right)\sin\left(\frac{2\pi}{c}z\right)=n$
IWP	$2\times\left(\cos\left(\frac{2\pi}{a}x\right)\cos\left(\frac{2\pi}{b}y\right)+\cos\left(\frac{2\pi}{b}y\right)\cos\left(\frac{2\pi}{c}z\right)+\cos\left(\frac{2\pi}{c}z\right)\cos\left(\frac{2\pi}{a}x\right)\right)-\cos\left(2\times\frac{2\pi}{a}x\right)\cos\left(2\times\frac{2\pi}{b}y\right)\cos\left(2\times\frac{2\pi}{c}z\right)=n$

$\boldsymbol{F}$ denotes the isosurface determined by the isosurface value n; a, b, and c denote the constants that control the TPMS unit dimensions in x, y, and z directions, respectively

strength and permeability, ensuring that they can withstand physiological loads while promoting rapid and robust bone healing [63]. This design flexibility makes TPMS-based implants highly versatile and effective for various clinical applications, offering a tailored approach to meet the diverse needs of patients with different bone defects and conditions. Parametric design methods for TPMS scaffolds with programmable pore size distributions have been proposed to effectively govern the pore size for practical application in bone implants [30].

The surface curvature of TPMS-based bone implants also plays a crucial role in their performance [64, 65]. The continuous and smooth curvature of TPMS structures (Fig. 2d) helps distribute stress more evenly across the implant, thereby reducing the likelihood of stress concentrations that could lead to mechanical failure [66]. This curvature enhances the mechanical compatibility of the implant with the natural bone, resulting in a more stable and durable integration. The surface curvature also influences cell behavior, with certain curvatures promoting better cell adhesion, proliferation, and differentiation. Surfaces that not only mimic the mechanical environment of natural bone but also support and enhance the biological processes necessary for successful bone regeneration and integration can be created by fine-tuning the curvature of TPMS-based implants [45].

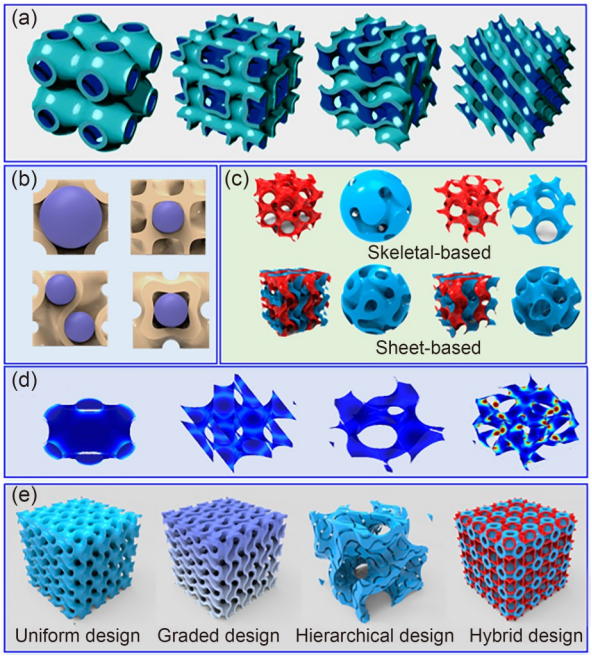

Fig. 2 TPMS-based structures. (a) Four types of TPMSs (reproduced from [67], Copyright 2017, with permission from Acta Materialia Inc.). (b) Pore size of TPMS-based structures (reproduced from [43], Copyright 2022, with permission from Elsevier). (c) Skeletal and sheet structures (reproduced from [30], Copyright 2020, with permission from the authors, licensed under CC BY). (d) Surface curvature of different TPMSs (reproduced from [66], Copyright 2017, with permission from IOP Publishing). (e) Four design strategies of TPMSs

This multifaceted approach makes TPMS-based implants a promising solution for advanced bone repair and replacement therapies.

Based on the flexibility and vast design space of TPMS structures, TPMS-based bone implants can be categorized into uniform, graded, hierarchical, and hybrid designs (Fig. 2e). The key difference among these designs lies in the strategies employed to vary the parameters during the design process, which aim to improve the performance of TPMS-based porous bone implants. The characteristics of these designs are discussed as follows.

2.2 Graded design

The graded design of TPMS-based bone implants involves the creation of structures with spatially varying properties that closely mimic the natural gradation observed in bone tissue (Fig. 3a). Unlike traditional uniform designs, graded designs allow continuous variation of the pore size, porosity, and structural properties of a single implant [68]. This approach enhances the implant's functionality and integration with the host bone. For TPMS-based bone implants, varying the porosity involves designing regions with different pore sizes and densities to optimize mechanical strength and biological integration, promoting better load distribution and enhanced tissue ingrowth. This can be achieved by spatially varying the design parameters in Cartesian space based on specific functions or tabulated data [69]. The graded design for bionic TPMS scaffolds can be achieved by analyzing computed tomography (CT) scans of human bones to determine the pore size and distribution [70].

The design of TPMS-based gradient structures involves several variables, including pore size, porosity, unit cell size, and wall thickness (Fig. 3b). By systematically varying these variables, it is possible to achieve the desired gradient design [71]. The most common gradient involves the uniform variation of these variables along a particular direction; however, they can vary exponentially to create more natural transitions. Typical gradient directions include linear and radial gradients [40]. Linear gradients exhibit consistent changes in variables along a straight line, whereas radial gradients exhibit changes radiating outward from central points. Radial gradients are particularly effective in mimicking the morphological variations of cylindrical bones [72].

Recent advances in the design of TPMS-based gradient structures have led to innovative approaches for mimicking the complex morphologies and mechanical properties of natural bone. Liu et al. [73] designed three distinct linear grading patterns for precise control over surface area and pore size and demonstrated their potential for mimicking host bone morphologies and mechanical properties. Wang et al. [74] proposed a centrosymmetric gradient structure in which the pore size and porosity are varied along an

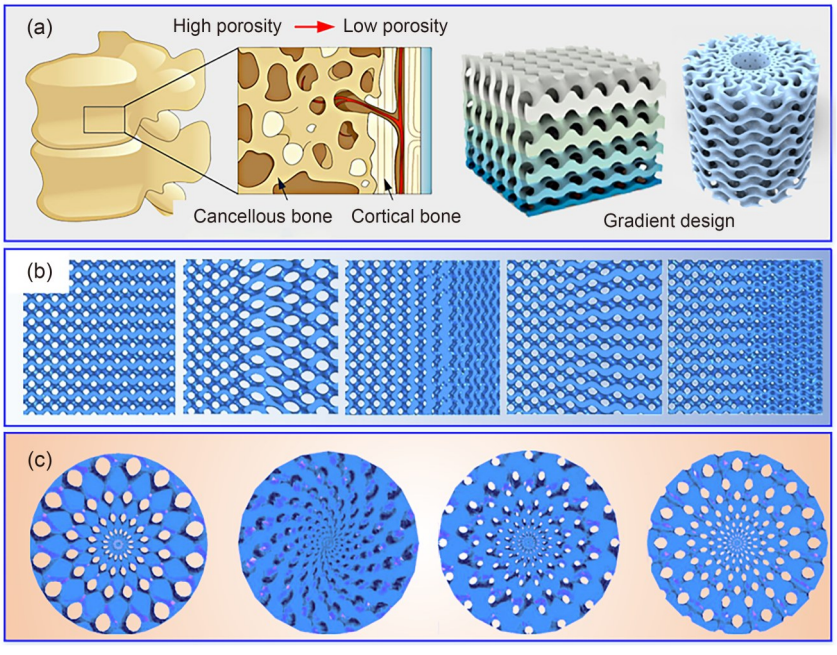

Fig. 3 Graded design of TPMS-based bone implants. (a) Gradient in human bone (reproduced from [31] (Copyright 2022, with permission from the authors, licensed under CC BY) and [76] (Copyright 2023, with permission from Elsevier)). (b) Linear gradient (reproduced from [71], Copyright 2019, with permission from Elsevier). (c) Radial gradient (reproduced from [81], Copyright 2020, with permission from Elsevier)

axisymmetric gradient. For radial gradients (Fig. 3c), Bora et al. [75] employed the gyroid TPMS lattice to parametrically design a functionally graded scaffold with radial grading to replicate the topology of human bone. Numerical investigations have shown that the designed scaffolds closely resemble human cortical bone and satisfy the essential structural requirements. Song et al. [76] proposed a radial-graded porosity design for low-modulus gyroid porous tantalum structures. They found that the radial-graded design exhibited a larger surface area with higher wall shear stress, which can activate cell growth factors and induce stress fiber formation.

For bone implants, the core of the implant should be designed with lower porosity to provide higher mechanical strength, whereas the outer regions may have higher porosity to facilitate bone ingrowth and vascularization [77]. Another approach involves varying the material composition within the implant, such as integrating metal alloys with density gradients or combining metals with bioactive hydrogels to create regions with distinct mechanical and biological properties [78]. Given the various gradient distributions present in actual bones, the design of TPMS-based bone implants can be guided by the real morphological and mechanical performance requirements of human bones [79]. This approach allows for the creation of implants that not only mimic the morphology and mechanical properties of natural bone but also ensure biocompatibility. Moreover, the performance of the implant and its integration with host tissue can be enhanced by tailoring the gradient design to match the specific structural and functional characteristics of the bone [80].

Some studies on biomimetic scaffold design have integrated TPMS structures and functionally graded porosity to enhance implant mechanical compatibility and biological integration with human bone tissue. For example, Zhang et al. [77] designed and optimized biomimetic scaffold architectures using TPMS structures to achieve mechanical matches with human bone tissues, particularly in load-bearing scenarios. Davoodi et al. [78] developed a functionally graded porosity hip implant by adjusting the local porosity at the implant/tissue interface to enhance the biological response. The gradual decrease in porosity from the surface to the center of the porous construct ensures both biological integration at the interface and mechanical integrity of the implant, providing a robust and biocompatible solution for bone tissue engineering.

2.3 Hierarchical design

Hierarchical design refers to the systematic organization of structural features at multiple scales, from macroscopic to microscopic levels [82]. In the context of bone implants, this approach involves creating a multilevel framework that closely replicates the complex architecture of natural bone (Fig. 4a). By integrating features at various scales, hierarchical design can better emulate the mechanical and biological properties of the bone, ensuring that the implant functions harmoniously within the body [32]. This design methodology

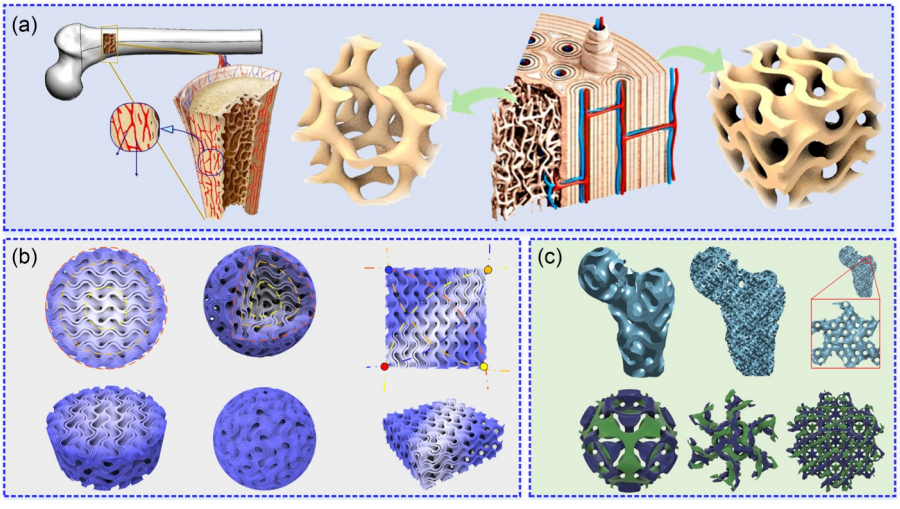

Fig. 4 Hierarchical design of TPMS-based bone implants. (a) Hierarchical pores in human bone (reproduced from [68] (Copyright 2022, with permission from the authors, licensed under CC BY) and [88] (Copyright 2022, with permission from Elsevier)). (b) Multisheet hierarchical design (reproduced from [32], Copyright 2020, with permission from the authors, licensed under CC BY). (c) Hierarchical sheet TPMS lattices (reproduced from [82] (Copyright 2021, with permission from CIRP) and [85] (Copyright 2019, with permission from Elsevier))

(Fig. 4b) is particularly advantageous in enhancing the performance and longevity of bone implants, as it allows for the optimization of strength and biocompatibility. The hierarchical design method based on TPMS offers significant potential benefits by accurately controlling the porosity and pore architecture gradients while preserving the inherent advantages of TPMS geometries [83].

A critical aspect of hierarchical design is the incorporation of multiple scales of porosity. In TPMS-based bone implants, varying the pore size across different scales can significantly impact mechanical stability and biological integration [33]. Larger pores at the macroscopic level facilitate the vascularization and nutrient flow necessary for tissue growth, whereas smaller pores at the microscopic level enhance the surface area required for cell attachment and proliferation. By carefully controlling the distribution and size of these pores, a scaffold that supports robust bone regeneration can be created while maintaining the necessary mechanical strength to withstand physiological loads. Zou et al. [84] proposed a hierarchical porous scaffold based on TPMS by adding small pores on the original TPMS structures to increase their versatility and controllability. Feng et al. [85] constructed hierarchical architectures using fractal-sheet TPMS and external freeform shapes through T-spline surfaces (Fig. 4c). The porosity features can be conveniently controlled in two-dimensional (2D) space according to actual CT images of human bones.

Natural bone exhibits a complex, multiscale architecture with varying degrees of porosity and density. By replicating this intricate structure, TPMS-based implants can achieve a closer resemblance to natural bone, both in form and function. Li et al. [86] proposed a Haversian system-like hierarchical structure with a pore size varying from the edge to the center. This biomimetic approach improves the mechanical compatibility of the implant and promotes bone regeneration. Luo et al. [87] introduced TPMS to metallic screws to address stress shielding and postoperative loosening in orthopedic fixation. They found that a stiffer integration between the screw and bone tissue could be achieved with more bone tissue regrowing on the inner surface of the hierarchical screw. Rezapourian et al. [88] designed anatomically matched implants composed of cortical bone mimicking Haversian and Volkmann canals combined with the trabecular-bone-mimicking parts with uniform internal TPMS structures. The optimal design could be achieved by combining pores with different scales to obtain a more successful integration and long-term functionality.

2.4 Hybrid design

Hybrid design refers to an innovative approach for integrating multiple TPMS geometries or combining TPMS structures with other types of structural elements [89, 90]. This approach leverages the strengths of various geometric configurations to create implants that are optimized for specific functional and mechanical requirements [91]. By blending different design elements, hybrid TPMS implants can achieve a superior balance of properties, thereby improving their overall performance and adaptability to medical applications. The TPMS-based hybrid design can be primarily categorized into two approaches. The first approach involves transitioning from one TPMS configuration to another, which is sometimes referred to as a heterostructure gradient in the literature [73]. By gradually changing the TPMS configuration, these implants can provide tailored mechanical properties and biological interactions across different regions

of the implant. The second approach involves fusing multiple TPMS units to adjust the performance of individual unit cells, such as enhancing the anisotropy [92]. This method enables precise control over the mechanical and biological properties of the implant at a microscale level, allowing for the customization of characteristics, such as stiffness, strength, and directional properties. Regions with distinct mechanical behaviors can be created by integrating different TPMS geometries within a single scaffold, thereby improving the overall versatility and functionality of the implant.

Several studies on heterostructure hybridizations have provided a foundation for the advancement of hybrid TPMS metamaterials. For example, Khaleghi et al. [90] proposed the idea of designing hybrid TPMS structures consisting of Schwarz-P/Neovius and each of the other five structures in laminated or matrix-spherical inclusion form to obtain structures with a more uniform directional elastic modulus. The mathematical functions of the hybrid structures were carefully parameterized to ensure a smooth transition between the two structures. They found that hybrid structures have a more uniform directional elastic modulus than their parent structures. They also demonstrated that an appropriate selection of the combination ratio of parent structures leads to the least universal anisotropy. Zhang et al. [93] used a similar approach to construct 1D, 2D, and 3D hybridizations using a Sigmoid function based on the P, IWP, and Forstner random dots (FRD) structures. Gao et al. [35, 94] proposed a periodic hybrid method for TPMS structures (Fig. 5a) while maintaining the original surface connectivity and structural strength. They used a representative volume element (RVE)-based homogenization method to demonstrate how hybridization expands the designable range of the elastic modulus. Li et al. [95] investigated the impact resistance of several hybrid structures when subjected to high strain-rate loading.

For the unit fusion method, Feng et al. [96] combined different TPMS units to acquire the appropriate elastic modulus and ideal isotropic properties using numerical homogenization theory and finite element analysis methods to build the relationship between the TPMS parameters and elastic modulus or anisotropy properties (Fig. 5b). A curvature-wall thickness adjustment method was proposed to achieve sheet TPMS structures with similar performances to the isotropic properties. Zhao et al. [89] used body-centered cubic and IWP lattice structures as internal and external structures, respectively, to construct interpenetrating lattice structures. They also developed a multiscale optimization framework to simultaneously optimize the distribution of the volume fractions and interpenetrating parameters.

Both hybrid design approaches significantly enhance the diversity and functionality of TPMS-based bone implants. The structural gradient method allows for the creation of implants with varying properties tailored to specific regions, ensuring optimal performance under physiological conditions. The fusion of multiple TPMS units enables detailed

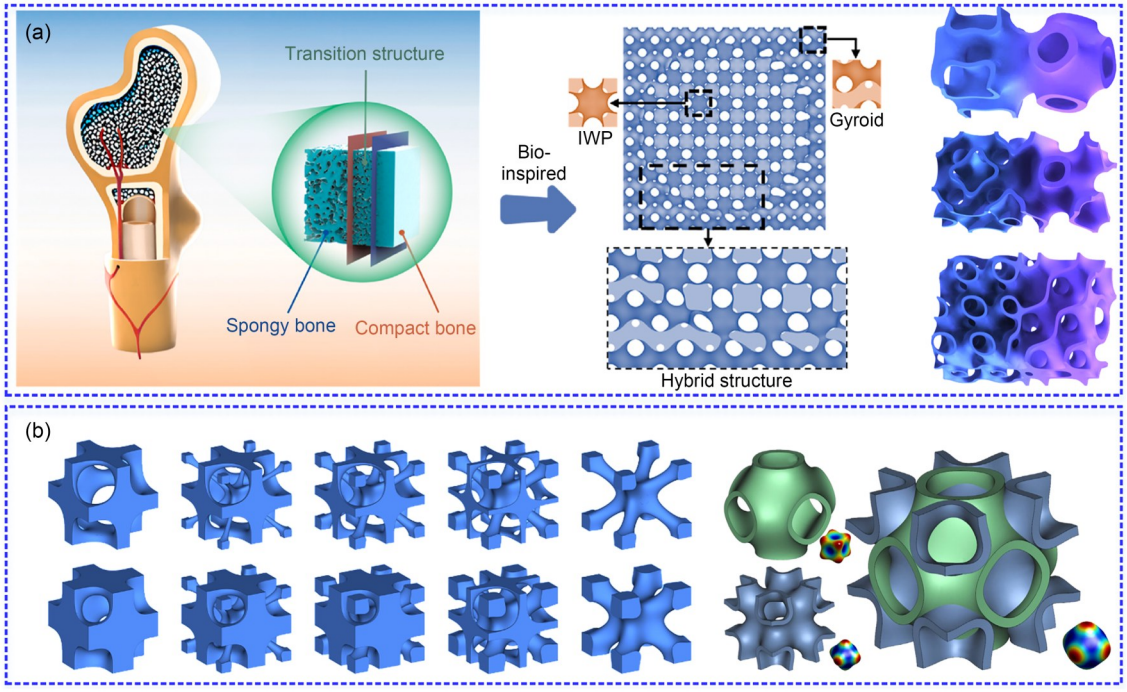

Fig. 5 Hybrid design of TPMS-based bone implants. (a) Transition hybrid design (reproduced from [94] (Copyright 2024, with permission from Elsevier) and [95] (Copyright 2023, with permission from Elsevier)). (b) Unit fusion hybrid design (reproduced from [89] (Copyright 2022, with permission from Elsevier) and [96] (Copyright 2021, with permission from the authors, licensed under CC BY))

customization of the mechanical properties, thereby promoting better integration with natural bone and improving the implant's ability to support tissue regeneration and load-bearing requirements. Overall, these hybrid design strategies represent a promising advancement in the development of next-generation bone implants, offering improved patient outcomes and broader clinical applications.

3 Fabrication of TPMS-based bone implants

The fabrication of TPMS-based bone implants that are characterized by complex and intricate internal structures, primarily relies on AM techniques. The application of AM in bone implants offers several advantages over traditional manufacturing approaches, including increased design flexibility for implant customization, reduced lead time for emergency cases, and the ability to create complex geometries for patient-specific implants. Given the versatility of AM techniques, this review categorizes the fabrication methods into three main types based on the materials used: metal-based, polymer-based, and ceramic-based TPMS implants. Metal-based TPMS implants typically employ techniques like LPBF to produce highly detailed and mechanically robust structures suitable for load-bearing applications. The resulting implants exhibit excellent strength and durability, closely matching the mechanical properties required for bone substitution. There is no fundamental difference in the processes used for different metals, and the different properties of the materials themselves are the key influencing factors for the design and surface modification strategies of bone implants. Therefore, this study focuses on introducing the material characteristics. Polymer-based TPMS implants often employ methods like FDM or SLA to create complex geometries at relatively low costs. Ceramic-based TPMS implants are fabricated using various AM techniques to create implants with excellent bioactivity and osteoconductivity, which are essential for bone regeneration. Ceramic implants offer a balance between mechanical strength and biological functionality, making them ideal for orthopedic and dental applications. Due to the relatively diversified preparation processes of ceramics, we will incorporate the preparation processes of different ceramic bone implants from research-development perspectives.

3.1 Metal-based bone implants

Metal-based AMs have attracted significant attention in the field of bone implants over the past decade. Materials that can be used for the metal-based AM of bone implants include titanium alloys, stainless steel 316L, magnesium (Mg) alloys, nickel–titanium alloys, and tantalum alloys. These materials are widely used in bone implants for different purposes. This review provides a comprehensive overview of these materials and their preparations for TPMS-based bone implants.

3.1.1 Titanium alloys

Titanium and its alloys, particularly Ti-6Al-4V, are highly favored for orthopedic joint replacements and dental implants because of their high strength-to-weight ratio and good biocompatibility [97, 98]. These materials are particularly chosen for their inertness toward tissues and body fluids, thereby ensuring a secure osseointegration [3]. The bioinertness of titanium is ensured by a protective film of titanium oxides that form spontaneously on its surface, which prevents the penetration of metal compounds and adheres well to the calcium and phosphate ions necessary for the formation of the mineralized bone structure [99, 100]. The ability of the alloy to be precisely fabricated into complex geometries using AM techniques (Fig. 6a) also enhances its suitability for customized implants [101]. This customization is crucial for patient-specific treatments to ensure better integration with existing bone structures and improve overall patient outcomes. Furthermore, the ongoing advancements in surface modification techniques for Ti-6Al-4V aim to enhance its osseointegration, which is the direct structural and functional connection between the living bone and the surface of a load-bearing implant, thereby promoting faster and more secure healing processes [102, 103].

Yan et al. [104] used selective laser melting (SLM) to manufacture Ti-6Al-4V gyroid and diamond TPMS lattices with interconnected high porosity (80%–95%) and pore sizes ranging from 560 to 1600 μm and from 480 to 1450 μm, respectively, for bone implants. The manufacturability, microstructure, and mechanical properties of these lattices were thoroughly evaluated. The mechanical properties of the fabricated TPMS structures matched the moduli of human bones, and this modification of the modulus and porosity helped reduce stress shielding and increase implant longevity. Ataee et al. [105] employed electron beam melting (EBM) to fabricate Ti-6Al-4V gyroid scaffolds (Fig. 6b) with anisotropic ratios comparable to those of trabecular bone, exhibiting a mixed mode of ductile and brittle behavior under compression. Tilton et al. [106] found that for a similar porosity and applied stress-amplitude, Schoen-IWP scaffolds exhibit significantly higher fatigue life when compared to the primitive (Fig. 6c). Wang et al. [74] created bone scaffolds with excellent mechanical properties, permeability, and cell adhesion capabilities using TPMS and Ti-6Al-4V. The results demonstrated the promising potential of the designed structures for use in artificial bone scaffolds. Therefore, the Ti-6Al-4V TPMS structures fabricated using AM techniques exhibited high porosity and tailored

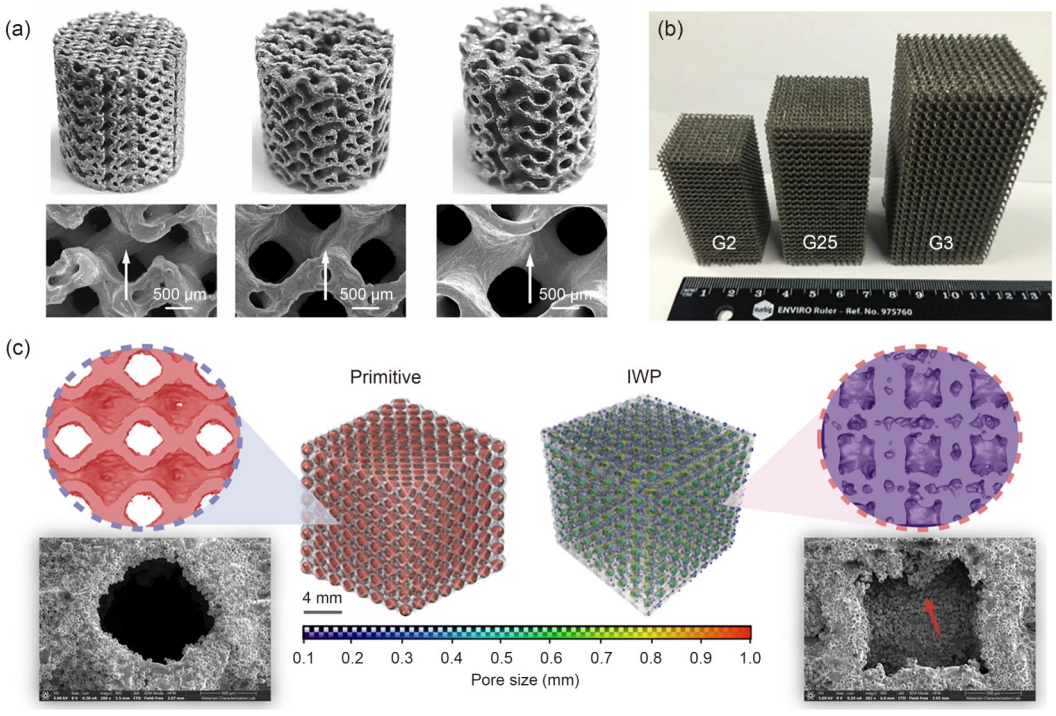

Fig. 6 Fabrication of Ti-6Al-4V TPMS structures for bone implants. (a) Microstructure of 3D-printed graded TPMS scaffolds (reproduced from [40], Copyright 2021, with permission from ASM International). (b) Gyroid scaffolds with different unit cell sizes manufactured by EBM (reproduced from [105], Copyright 2017, with permission from Elsevier). (c) Structural and morphological evaluation of the additively manufactured TPMS scaffolds (reproduced from [106], Copyright 2023, with permission from the Society of Manufacturing Engineers)

mechanical properties resembling human bone. This design flexibility helps mitigate stress shielding and improves implant durability, making these implants promising candidates for advanced bone implants.

Several researchers have proposed process improvements and enhancements to better utilize the fabricated Ti-6Al-4V TPMS structures for bone implants, focusing on their mechanical properties, biocompatibility, stress-shielding mitigation, and fatigue performance. For example, Rezapourian et al. [107] explored Ti-6Al-4V split-P TPMS structures manufactured using SLM and evaluated two cell morphologies with varying densities. They found that the elastic modulus, yield strength, and strength of the fabricated parts approached the mechanical properties of the trabecular and cortical bone. Liao et al. [40] fabricated Ti-6Al-4V scaffolds with radial gradient porosity distributions using SLM to mimic natural bone structures. The scaffolds exhibited varying porosities (55%–71%) and pore sizes (333–674 μm), with mechanical properties (Young's modulus: 2.7–7.4 GPa; yield strength: 233–520 MPa) suitable for orthopedic applications. Biocompatibility was demonstrated by performing cell viability assays. Song et al. [11] proposed porous root analog implants of Ti-6Al-4V using TPMS structures to mitigate stress shielding and promote osteoblast growth. Compression experiments and finite element analysis demonstrated that implants with 30% and 40% porosity effectively prevented stress shielding, enhanced bone tissue integration, and optimized clinical implantation outcomes. Tilton et al. [106] investigated the fatigue performance of Ti-6Al-4V scaffolds designed using TPMS, highlighting the impact of structural design and manufacturing variability on metabiomaterials. They found that the Schoen-IWP scaffold exhibited a 97% higher fatigue life than the primitive scaffold. The primitive scaffolds closely replicated the compressive mechanical properties of the trabecular bone.

3.1.2 Stainless steel 316L

Stainless steel is another prominent material used in AM for TPMS-based bone implants because of its favorable mechanical properties, biocompatibility, and cost-effectiveness [108]. Known for its excellent corrosion resistance and strength, stainless steel 316L is particularly suited for medical applications where durability and reliability are critical [109]. The application of stainless steel 316L in AM allows for the creation of intricate TPMS structures (Fig. 7a) that closely mimic the porosity and mechanical properties of natural bone, thereby promoting better osseointegration and tissue ingrowth. Despite its advantages, one of the challenges with stainless steel 316L is its relatively high elastic modulus compared to natural bone, which can lead to stress shielding. However, advancements in AM techniques have enabled the production of optimized porous structures that can

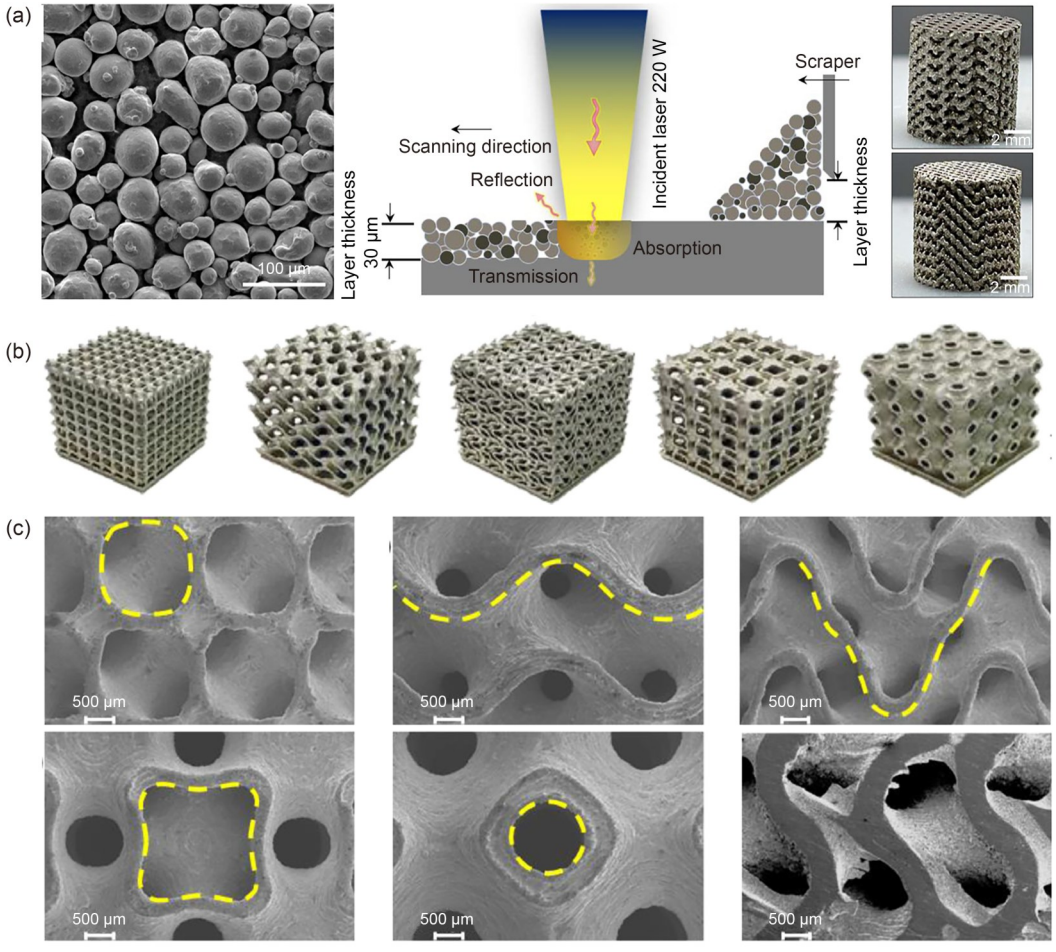

Fig. 7 Fabrication of stainless steel TPMS structures for bone implants. (a) SLM process for the fabrication of stainless steel lattice structures, including the powder and fabricated TPMS structures (reproduced from [114] (Copyright 2023, with permission from the authors, licensed under CC BY) and [115] (Copyright 2024, with permission from Elsevier)). (b) Fabricated TPMS lattice structures using stainless steel 316L (reproduced from [109], Copyright 2023, with permission from Elsevier). (c) SEM images of fabricated surfaces (reproduced from [109], Copyright 2023, with permission from Elsevier). SEM: scanning electron microscope

mitigate this issue, making stainless steel 316L a viable option for producing effective and long-lasting TPMS-based bone implants [110].

Wang et al. [111] compared the mechanical properties and cytotoxicity of TPMS gyroid and other porous structures fabricated from stainless steel 316L using SLM at various relative densities. They found that TPMS structures exhibit favorable Young's modulus and excellent biocompatibility, highlighting their potential for biomedical applications. Szatkiewicz et al. [112] investigated the mechanical properties and energy absorption capabilities of cylindrical TPMS structures with shell gyroid unit cells fabricated from stainless steel 316L under compression loading. Ravichander et al. [109] evaluated the mechanical and electrochemical properties of sheet-based TPMS lattices (Figs. 7b and 7c) fabricated from stainless steel 316L, revealing enhanced corrosion resistance compared to solid samples and offering valuable insights for biomedical applications. Ma et al. [113] examined the suitability of stainless steel 316L gyroid structures for bone scaffolds by analyzing their mechanical properties and fluid dynamics. They found that increasing the volume fraction improved the elastic moduli and yield stresses and that the fluidity of the structures enhanced nutrient transport. These studies confirmed that stainless steel 316L TPMS structures exhibit excellent mechanical properties, corrosion resistance, and biocompatibility, making them promising for various biomedical applications.

Foroughi et al. [116] fabricated TPMS scaffolds for bone tissue engineering using stainless steel 316L to ensure that these scaffolds possess essential mechanical strength and biocompatibility, thereby highlighting the suitability of the material for optimizing bone scaffold architectures. Cui et al. [115] created four TPMS structures using stainless steel 316L by incorporating TiB_2 nanoparticles to enhance their mechanical properties. This nanocomposite exhibited improved nano-hardness, ultimate compressive stress, and

Young's modulus compared to plain stainless steel, closely matching the human cortical bone strength. Zhu et al. [117] employed Schwarz primitive TPMS to design novel porous scaffolds, optimizing the scaffold thickness to enhance its mechanical and biological properties. The experimental and numerical results confirmed the enhanced mechanical performance and controlled permeability of the scaffold, demonstrating the effectiveness of the method in tailored scaffold design for biomedical applications. Yang et al. [118] studied the compression–compression fatigue behavior of gyroid cellular structures and revealed enhanced fatigue resistance after sandblasting treatment, which was characterized by reduced cyclic ratcheting and improved high-cycle fatigue performance. These studies underscore the versatility of stainless steel 316L for fabricating TPMS scaffolds with enhanced mechanical properties and biocompatibility, highlighting its potential for advancing bone implant applications.

3.1.3 Mg alloys

Mg and its alloys are emerging as prime candidates for AM of TPMS-based bone implants because of their exceptional physical properties and biocompatibility [119, 120]. Known for their low density, high specific strength, and stiffness, Mg alloys (Fig. 8a) have been widely used in aerospace and automotive industries as structural metals [121]. Their application in the biomedical field is particularly promising because of their excellent biocompatibility, good osseointegration properties, biodegradability, and elasticity that closely match human bone, thereby reducing the risk of stress shielding [122]. This makes Mg alloys ideal for orthopedic implants. Moreover, Mg-based implants must feature specific geometries that match critical-sized bone defects and highly porous, interconnected structures to facilitate the delivery of nutrients, cells, proteins, and growth factors, thereby promoting bone ingrowth [123].

Temiz et al. [124] employed a casting technology based on infiltration to fabricate controllable porous Mg alloy gyroid structures that were subjected to mechanical testing. They found that Young's modulus of these gyroid structures fell within the range of human trabecular bone but was lower than that of sheep bone, as determined through compression tests and finite element analysis. Ren et al. [125] developed a novel vat photopolymerization-assisted template replacement method for creating intricate TPMS structures with various pore sizes in biodegradable Zn-based porous scaffolds. The resulting Zn–1Mg scaffolds exhibited precise pore structures with a deviation of less than 2% from

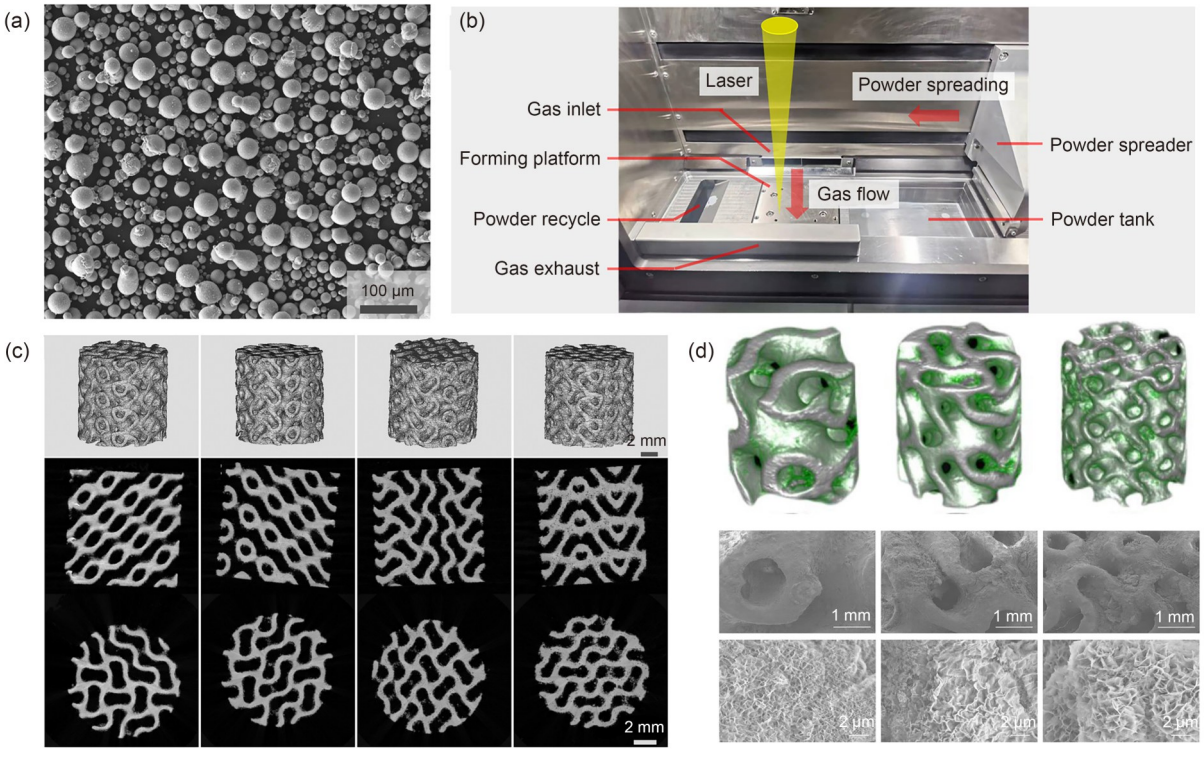

Fig. 8 Fabrication of Mg TPMS structures for bone implants. (a) SEM image of WE43 Mg alloy powder (reproduced from [126], Copyright 2022, with permission from the authors, licensed under CC BY-NC-ND). (b) Setup of the AM processing chamber (reproduced from [126], Copyright 2022, with permission from the authors, licensed under CC BY-NC-ND). (c, d) Formation quality of TPMS-based porous scaffolds by macroscopic and cross-sectional images using μ-CT (reproduced from [126] (Copyright 2022, with permission from the authors, licensed under CC BY-NC-ND) and [127] (Copyright 2023, with permission from the authors, licensed under CC BY-NC-ND)). SEM: scanning electron microscope

the designed porosity, demonstrating excellent mechanical properties, cytocompatibility, and antibacterial activity. These non-AM techniques exemplify effective methods for fabricating precise and functional porous Mg structures.

AM has significantly facilitated the preparation of porous Mg alloy structures, offering great potential for advanced biomedical applications (Figs. 8b and 8c). For example, Wang et al. [127] investigated the effects of pore size in additively manufactured biodegradable porous Mg scaffolds (Fig. 8d) on mechanical properties, biodegradation, and new bone formation. They found that scaffolds with smaller pore sizes exhibited superior mechanical properties, enhanced osteogenic differentiation, and promoted new bone formation, particularly when high-temperature oxidation was applied to improve corrosion resistance. They also examined the influence of the layer thickness on the formation quality, microstructure, mechanical properties, and corrosion resistance of the WE43 Mg alloy and found that increased layer thickness led to enhanced tensile strength and elongation but higher corrosion rates due to more precipitation phases [126]. They also investigated the optimization of LPBF parameters for WE43 Mg alloy porous scaffolds, achieving high structural fidelity and mechanical strength comparable to cancellous bone while demonstrating promising biocompatibility and initial osteogenic effects despite challenges in controlling degradation rates [128]. Yue et al. [129] explored AM of high-porosity Mg alloys for structural and biomedical applications based on TPMS and found that the structures exhibit interconnected architectures and porosity-dependent properties, with elastic moduli akin to cancellous bone.

3.1.4 Nickel–titanium alloys

Nickel–titanium (Ni–Ti) alloys are highly suitable for AM in TPMS-based bone implants because of their shape memory effect, superelasticity, and high damping capacity [130]. These properties enable the Ni–Ti alloys to recover their shape under stress-free conditions, exhibit large nonlinear recoverable strains, and efficiently dissipate energy as heat, thereby enhancing their energy absorption and mechanical resilience. These characteristics improve the durability, adaptability to dynamic body loads, and patient comfort of bone implants by mitigating vibrations [131]. AM techniques allow precise control over the complex porosity and pore architecture of Ni–Ti TPMS structures (Fig. 9) [132, 133], thereby promoting osseointegration and bone tissue growth and making Ni–Ti alloys a promising material for advanced orthopedic implants [134, 135].

Recent advances in AM have greatly enhanced the design and fabrication of Ni–Ti porous scaffolds. For example, Lv et al. [136] designed several porous scaffolds based on TPMS with consistent porosity but varying pore strategies using a novel Ni46.5Ti44.5Nb9 alloy and SLM technique. They systematically investigated the effects of

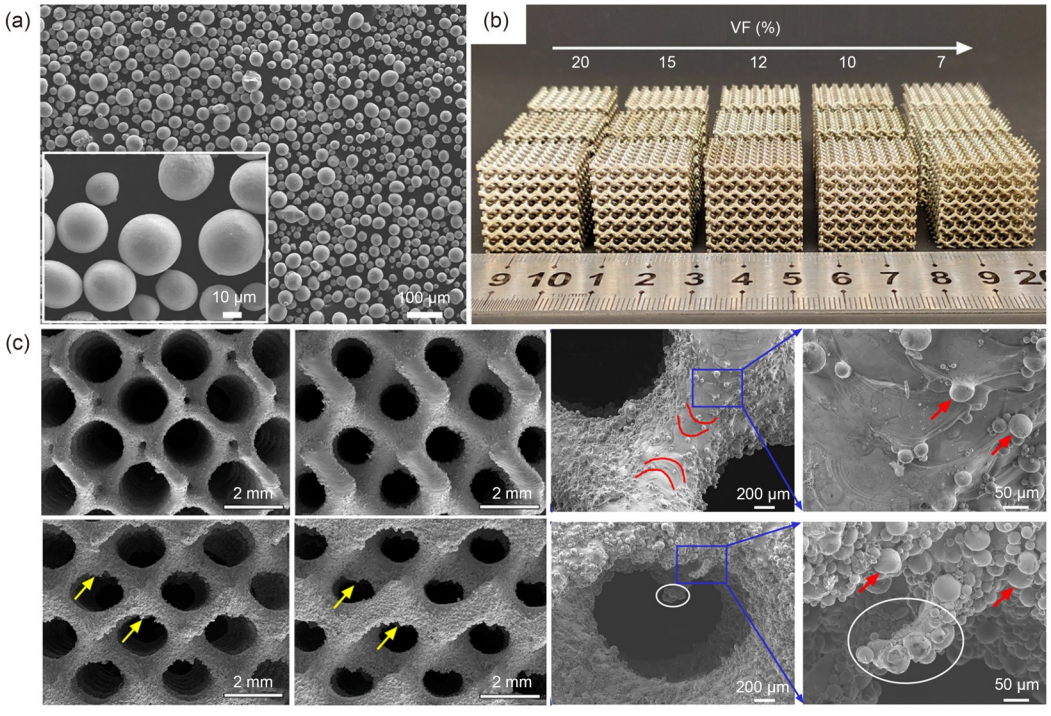

Fig. 9 Fabrication of Ni–Ti TPMS structures for bone implants (reproduced from [132], Copyright 2022, with permission from Elsevier): (a) SEM images of the Ni–Ti powder; (b) additively fabricated Ni–Ti gyroid TPMS lattice structures; (c) SEM images of the Ni–Ti TPMS lattice structures. VF: volume fraction; SEM: scanning electron microscope

these pore strategies on the microstructure, mechanical properties, and permeability of scaffolds. They found that although the pore size had little effect on the mechanical properties, increasing the pore size significantly improved the permeability because of decreased specific surface areas. Sun et al. [137] designed three types of porous Ni–Ti structures based on TPMS and demonstrated that AM is an efficient method for producing highly accurate porous Ni–Ti TPMS structures. They found that porous Ni–Ti TPMS structures offer reversible compressibility, rapid elastic recovery, and controllable shape memory recovery, making them highly efficient energy-absorbing structures. Hussain et al. [138–140] addressed the challenges of machining Ni–Ti alloys using conventional methods because of their high ductility and strength, highlighting the advantages of AM in overcoming these limitations. They comprehensively analyzed the geometric properties and process parameters of the microstructural properties and solid-phase distribution within the samples. Their findings revealed significant impacts of the process parameters and structural topology on the microstructural features, including Ni evaporation and the formation of oxide- and Ti-rich phases. These studies underscore the potential of intricate TPMS geometries in Ni–Ti alloys, suggesting their potential for innovative applications and advancements across various fields.

Several attempts have been made to fabricate more complex structures and higher-performance porous scaffolds for bone implants. For example, Zhang et al. [141] explored additively manufactured Ni–Ti lattice structures, highlighting their controllable bio/mechanical properties, large deformation capacity, and damping characteristics akin to natural bone, making them highly suitable for bone implantation applications. Tang et al. [142] highlighted the unique combination of the porous metal characteristics and shape memory properties. They emphasized the significant impact of cyclic loading on the phase transformation and plastic deformation in these materials compared to bulk Ni–Ti alloys. Jin et al. [143] explored Ni–Ti alloys based on TPMS lattice metamaterials, focusing on varying interlacing-cell numbers within gyroid lattice structures. Their findings provide insights into optimizing interlacing configurations to balance manufacturability with mechanical and hyperelastic performance. Zhang et al. [144] designed several TPMS-based gradient porous structures to demonstrate the integration of metallurgical and architectural design principles as a novel approach to tailoring the mechanical properties of gradient porous metals for advanced applications.

3.1.5 Tantalum alloys

Tantalum metal has emerged as a promising biomaterial, exhibiting superior biocompatibility and inherent antibacterial properties [145]. The surface tantalum pentoxide oxide layer confers exceptional biological inertness, whereas the terminal hydroxyl groups facilitate hydroxyapatite (HA) deposition, thereby promoting osseointegration at the bone–tantalum interface [76, 146]. The elastic modulus of porous tantalum aligns closely with that of human trabecular and cortical bone, mitigating the stress shielding effects and enhancing bone remodeling [147]. The high friction coefficient of the implants compared with those of cancellous and cortical bone bolsters the interfacial bonding with the host bone, thereby augmenting the initial implant stability [5]. Due to the high melting point and high affinity for oxygen of tantalum, traditional processing methods are difficult to process with low production efficiency and material utilization, which increases the preparation cost of tantalum implant devices. Porous tantalum (Figs. 10a and 10c) is commonly processed by vapor deposition or powder metallurgy processes [148, 149]. Clinically, porous tantalum has been widely used in joint arthroplasty, bone defect repair, and spinal fusion procedures [76, 150]. In hip and knee arthroplasties, porous tantalum-constructed integrated acetabular cups and reinforcement pads have exhibited commendable stability both initially and over the long term [150, 151].

Building on these attributes, Balla et al. [5] employed laser-engineered net shaping to fabricate porous tantalum structures with variable porosity for the first time. The mechanical properties of these structures, including a tailored Young's modulus ranging from 1.5 to 20 GPa, can be adjusted by modifying the pore volume fraction. In vitro biocompatibility tests revealed superior cellular adherence, growth, and differentiation in the porous tantalum structures compared with porous Ti control structures, indicating the potential for enhanced and early biological fixation. The improved in vitro cell–material interactions on porous tantalum are attributed to its chemistry, high wettability, and greater surface energy compared to porous titanium.

Expanding their manufacturing capabilities, Soro et al. [147] successfully produced biomimetic Ti–tantalum bone scaffolds using the LPBF process. These scaffolds, designed with TPMS architectures, maintained their morphological characteristics postmanufacturing and exhibited compressive mechanical properties suitable for use as bone implant substitutes. In vitro cell cultures confirmed the high biocompatibility of these novel biomaterials, with the interconnected open-pore designs showing improved biological responses.

To further enhance the functionality of these implants, Song et al. [76] introduced a radial gradient design for the fabrication of low-modulus gyroid porous tantalum structures using LPBF AM (Fig. 10b). This design enhances the mechanical properties and permeability of structures, thereby promoting optimal biological performance. The radial gradient design increased the elastic modulus and yield strength due to edge strengthening, whereas the permeability increased with porosity, which is consistent with the

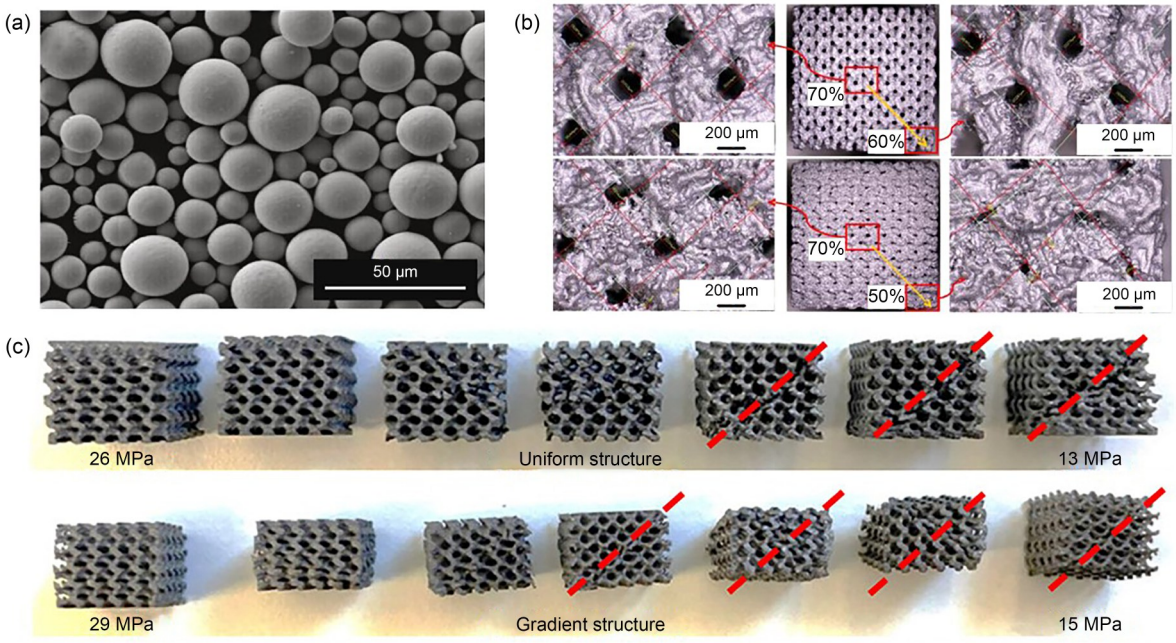

Fig. 10 Fabrication of tantalum TPMS structures for bone implants. (a) SEM image of the tantalum powder (reproduced from [151], Copyright 2014, with permission from Acta Materialia Inc.). (b) Additively fabricated tantalum gyroid TPMS lattice structures (reproduced from [76], Copyright 2023, with permission from Elsevier). (c) Fatigue deformation mode for the uniform and gradient tantalum gyroid TPMS structures (reproduced from [145], Copyright 2021, with permission from Elsevier). SEM: scanning electron microscope

range of cancellous bone permeability. This feature is especially beneficial for nutrient transportation and cell migration, which are crucial for the biological performance of bone implants. The innovative work of Chen et al. [152] further enhances tantalum's role in bone implants by designing and manufacturing gyroid tantalum structures with functional gradients in density and cell size using LPBF. The density gradient structures provide improved impact resistance, whereas the cell-size gradient structures enhance nutrient and gas transport due to lower inlet pressure and increased wall shear stress, underscoring the promise of these designs for superior osseointegration and biological performance in bone implant applications.

To regulate the TPMS structure, Wei et al. [153] employed SLM technology to fabricate gyroid porous tantalum structures, which were then filled with chitosan (CHS) and nano-HA (n-HA) composite sponges prepared by freeze-drying. This innovative approach resulted in a composite scaffold that combines the mechanical strength and corrosion resistance of porous tantalum with the bioactivity and osteoinductivity of the CHS/n-HA composite. These scaffolds offer a comprehensive solution as an ideal substitute for bone defect repair.

3.2 Polymer-based bone implants

Polymer-based biomaterials have been used in the human body since the invention of synthetic polymers. Clinical practice has adopted these materials because of their robust, inert, and biocompatible nature, which facilitates the management of injured or infected bone, thereby enhancing patient outcomes. Polymer biomaterials can be applied to various tissues, including cardiovascular, neural, musculoskeletal, and dermal tissues [39, 154]. Polymer-based TPMS implants (Fig. 11c) are commonly fabricated using FDM or SLA to achieve precise geometries and intricate structures in a cost-effective manner. These methods enable engineers to create implants with tailored porosity and surface characteristics, which are critical for promoting tissue integration and healing in biomedical applications [155, 156]. The flexibility of polymer materials allows for the fabrication of designs that mimic the natural properties of bone for providing mechanical support.

Material extrusion-based AM, commonly known as FDM, is the predominant technique for fabricating polymer-based structures [157, 158]. This method involves layer-by-layer deposition of thermoplastic polymers to construct complex geometries directly from digital models. Due to its versatility, cost-effectiveness, and ease of use, FDM has been widely used in both prototyping and the production of functional parts [159–161]. Al Hashimi et al. [162] fabricated polymer TPMS sheet lattices with 70% porosity using a pneumatic material extrusion method. The printed scaffolds demonstrated high print accuracy with minimal percentage errors of less than 15% and significant improvements in cell proliferation and attachment. Sabahi et al. [163]

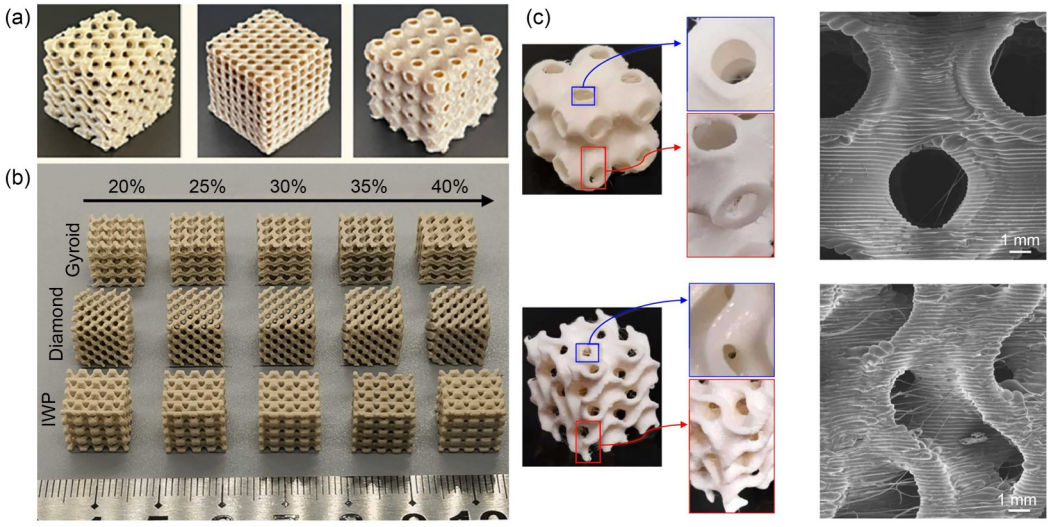

Fig. 11 Fabrication of polymer-based TPMS structures for bone implants. (a) PEEK TPMS structures fabricated by material extrusion-based AM (reproduced from [163], Copyright 2024, with permission from the authors, licensed under CC BY). (b) PEEK TPMS structures fabricated by LPBF (reproduced from [171], Copyright 2022, with permission from Elsevier). (c) SEM images of the TPU-based TPMS lattice structures (reproduced from [172], Copyright 2022, with permission from Elsevier). SEM: scanning electron microscope; TPU: thermoplastic polyurethane

used material extrusion-based AM to fabricate density-graded TPMS polyether ether ketone (PEEK) scaffolds (Fig. 11a), which achieved graded porosity, mirroring the natural bone microstructure, and demonstrated superior mechanical properties with the gradient gyroid scaffold exhibiting elastic modulus and strength of 200 and 5.15 MPa, respectively. Du et al. [164] fabricated 3D-printed PEEK/silicon nitride (PEEK/SiN) scaffolds with a TPMS structure, offering advantages like a large surface area and uniform stress distribution. The 30% porosity scaffold exhibited mechanical properties similar to those of trabecular bone, with a compressive strength of (34.56±1.91) MPa and elastic modulus of (734±64) MPa, demonstrating favorable damping properties. Tripathi et al. [165] fabricated some gyroid scaffolds with varying porosities using FDM with polylactic acid (PLA) filaments, showing compressive strength equivalent to human trabecular bone and expected biocompatibility in vitro. Oladapo et al. [166, 167] developed a PEEK and calcium HA (cHAp) composite with TPMS structures to optimize dental implants. The optimized structures were fabricated using FDM and resulted in increased stiffness and improved fundamental frequency, demonstrating the potential of PEEK composites as lightweight and biocompatible alternatives to metal implants in dental applications. Alkebsi et al. [168] used TPMS and FDM to design and fabricate lightweight orthopedic implants, which were consistent with cancellous bone properties in elastic modulus and porosity ratio. Guo et al. [169] used FDM to develop TPMS structural PLA/graphene oxide (GO) scaffolds, which exhibited improved mechanical properties, with the addition of 0.1% GO increasing the tensile and compression moduli by 35.6% and 35.8%, respectively. The cells showed better adhesion, proliferation, and osteogenic differentiation in bone marrow stromal cells. Agarwal et al. [170] used TPMS to design biomimetic scaffolds with varying unit cell sizes, which were fabricated using FDM with PLA. These findings suggest that polymer-based TPMS scaffolds fabricated using material extrusion-based AM can be tailored to optimize mechanical strength for bone tissue engineering applications.

In addition to material extrusion-based AM, other AM methods, such as SLA or LPBF, have been used to fabricate polymer-based TPMS structures intended for bone implant applications. Lumba et al. [173] investigated the permeability of a biological implant structure, focusing on a gyroid lattice design that mimics the trabecular bone architecture. The designed TPMS structures were fabricated using DLP to experimentally assess the fluid flow permeability. The experimental results were compared with the numerical predictions to understand the permeability properties, highlighting the discrepancies and suggesting avenues for implant design and fabrication improvement. Abueidda et al. [156] used LPBF to create different polymeric TPMS cellular structures and compared their performances. The results showed that the Neovius and IWP exhibited higher stiffness and strength than primitive, with the mechanical properties affected by the specimen size. Wang et al. [171] designed porous PEEK scaffolds with a highly tunable elastic modulus using TPMS structures (Fig. 11b), which were then fabricated via LPBF. The fabricated gyroid scaffolds exhibited the lowest manufacturing deviation and optimal mechanical properties, with elastic moduli ranging from 42.17 to 512.12 MPa, comparable to human trabecular bones. Gabrieli et al. [174] designed several porous scaffolds with

TPMS geometries, which were then 3D-printed using a stereolithographic technique with dental resin. These scaffolds exhibited mechanical properties and pore interconnectivity comparable to those of cancellous bone.

3.3 Ceramic-based bone implants

Ceramics, comprising inorganic and nonmetallic solids like oxides, nitrides, carbides, and borides, transform into bone-like structures when exposed to high temperatures because of the formation of ionic and covalent bonds [175]. These materials have been widely used in bone scaffolds because of their high tensile strength and ability to form stable bonds with host tissues. Traditional methods for fabricating ceramic scaffolds struggle to produce intricate geometries and interconnecting porous structures due to the rigidity and fragility of ceramics. In contrast, AM offers a promising solution for fabricating complex geometries and shapes that are difficult to achieve with conventional techniques, allowing for the creation of biocompatible, chemically resistant, high-strength, and thermally conductive ceramic scaffolds [176]. Various AM strategies, including material extrusion-based AM, SLA, and DLP, are widely used to fabricate bone scaffolds for tissue engineering and clinical research applications [177]. This review discusses these AM techniques for fabricating ceramic-based TPMS structures for bone implants from a process perspective.

Similar to the preparation of polymer-based TPMS structures, material extrusion-based AM has been widely used to fabricate complex ceramic structures [176]. The main advantage of this method lies in its ability to extrude materials that can be melted or processed into a flowable state and subsequently shaped into the desired structure [178]. It is worth noting that the performance (including quality and mechanical properties) of the structures fabricated using this stepwise extrusion and accumulation process is significantly influenced by various planning parameters, such as path spacing and layer thickness. Moreover, very fine structures like TPMS, which consist of curved surfaces, present additional challenges during fabrication. Consequently, while there is substantial research on using material extrusion-based AM to fabricate ceramic porous scaffolds [179], studies focusing on the preparation of TPMS structures using this method are still relatively limited.

Baumer et al. [180] presented an open-source software algorithm for creating 3D-printable Fischer–Koch S (FKS) and a gyroid scaffold, demonstrating the successful fabrication of HA FKS scaffolds (Fig. 12a) using a low-cost AM method. The results showed promising dimensional accuracy, internal microstructure, and porosity characteristics for TPMS-based ceramic scaffolds for bone regeneration. Restrepo et al. [181] used an FDM printer to create ceramic structures with gyroid, Schwarz primitive, and Schwarz diamond surfaces (Fig. 12b), which were suitable for bone tissue scaffolds. They compared their mechanical properties to determine the optimal TPMS for constructing ceramic scaffolds for bone repair. All geometries exhibited porosities within the range of the trabecular bone. Among the geometries, the Schwarz primitive exhibited the best mechanical behavior, which was attributed to the orientation of the columns supporting the load. Charbonnier et al. [182] produced custom-made gyroid structure implants (Fig. 12c) with and without cortical-like reinforcement using sintered HA and material extrusion-based AM and characterized their morphological, physicochemical, and mechanical features. The results showed that the implants had improved stiffness and fracture resistance, concentrating new bone formation in the implant core without affecting bone quantity or maturity.

In the vat polymerization process, such as SLA and DLP, a photocurable liquid polymer is selectively solidified by a low-power ultraviolet light source at the surface of a vat. The build progresses as the z-axis descends, with each layer of the liquid polymer spreading over the previously solidified surface until the entire object is formed. In recent years, these AM methods have been extensively used to fabricate ceramic bone implants, offering several advantages. These technologies enable the creation of intricate and highly customized structures that are difficult to achieve using traditional manufacturing techniques. These methods also allow for precise control over porosity, which is crucial for promoting bone ingrowth and integration. Moreover, the ability to fabricate complex geometries enhances the functionality and performance of implants, thereby ensuring better patient outcomes.

Kong et al. [183] developed a method for fabricating high-strength and high-toughness TPMS-based ceramic structures by optimizing the SLA process and exploring graded configurations. The results showed significant improvements in toughness and energy absorption compared to pure ceramics. Zhang et al. [184] fabricated gyroid β-tricalcium phosphate (β-TCP) bioceramic scaffolds using SLA to mimic cancellous bone architecture. These scaffolds exhibited adjustable porosity, pore size, wall thickness, and compressive strength and can be tailored to suit various bone sites. The fabricated ceramic gyroid structures enhanced cell proliferation and showed promise for efficient repair of bone defects. Li et al. [36] focused on enhancing bone defect repair using bioactive glass-β-tricalcium phosphate (BG-TCP) scaffolds with TPMS structures fabricated via SLA. The incorporation of BG improved the compressive strength of the β-TCP matrix, facilitating adaptable biodegradability, and promoting the osteogenic differentiation of bone marrow mesenchymal stem cells (BMSCs) and angiogenic ability of endothelial progenitor cells. Based on the above studies, the optimization of the SLA processes

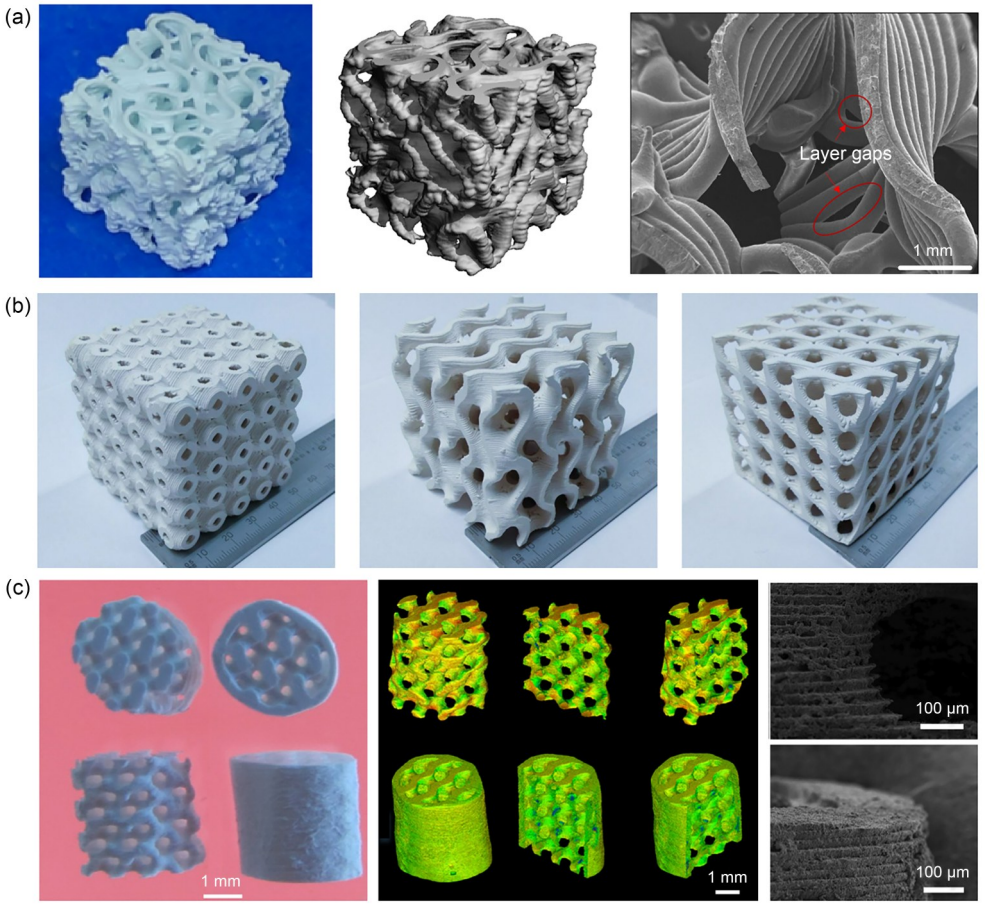

Fig. 12 Fabrication of ceramic-based TPMS structures using material extrusion-based AM. (a) HAp FKS scaffold and its microstructure characterization (reproduced from [180], Copyright 2023, with permission from the authors, licensed under CC BY). (b) Ceramic scaffolds with different TPMS geometries (reproduced from [181], Copyright 2017, with permission from the authors, licensed under CC BY). (c) Gyroid-based macroporous bioceramic implants (reproduced from [182], Copyright 2020, with permission from Acta Materialia Inc.)

and incorporation of bioactive glass significantly enhanced the mechanical properties and biological performance of the TPMS-based ceramic scaffolds for bone implants.

HA is ideal for bone implants because of its biocompatibility and chemical similarity to natural bone minerals. This enables the fabrication of customized implants (Fig. 13d) with tailored mechanical properties and complex geometries, enhancing osseointegration and long-term implant stability [185]. Bouakaz et al. [186] explored the fabrication and evaluation of HA scaffolds with a gyroid-TPMS porous structure using DLP (Fig. 13c). The scaffolds designed to mimic trabecular bone exhibited high porosity (65%) and excellent HA densification (90.5%). Mechanical testing revealed suitable properties for guided bone regeneration at nonload-bearing sites, such as in maxillofacial contour reconstruction. This pilot study underscores the potential of TPMS-based scaffolds for clinical bone regeneration applications. Maevskaia et al. [187] used TPMS microarchitectures, including diamond, gyroid, and primitive designs, for 3D printing using HA for bone tissue engineering. Mechanical testing revealed superior strength of the diamond and gyroid structures compared to the primitive. In calvarial defect and bone augmentation models, gyroid demonstrated significantly enhanced osteoconduction and bone ingrowth compared with primitive implants, highlighting its potential as a favorable TPMS-based scaffold for treating bone deficiencies in clinical applications. Liang et al. [188] used DLP to fabricate HA scaffolds with different porous structures, which were then investigated in terms of compressive properties and cell metabolism to analyze their potential in bone tissue engineering applications. Yao et al. [189] investigated the potential of DLP-printed HA ceramics with TPMS geometries, enhanced by wet CO_2 sintering, as promising materials for bone engineering applications. Deng et al. [37] proposed functional gradient lattice structures based on TPMS designs and fabricated them using DLP with a consistent porosity of 65% (Fig. 13b). Four gradient scaffolds were investigated, and the results revealed that the gradient structures significantly enhanced the compressive strength compared to the uniform structures. Hua et al. [190]

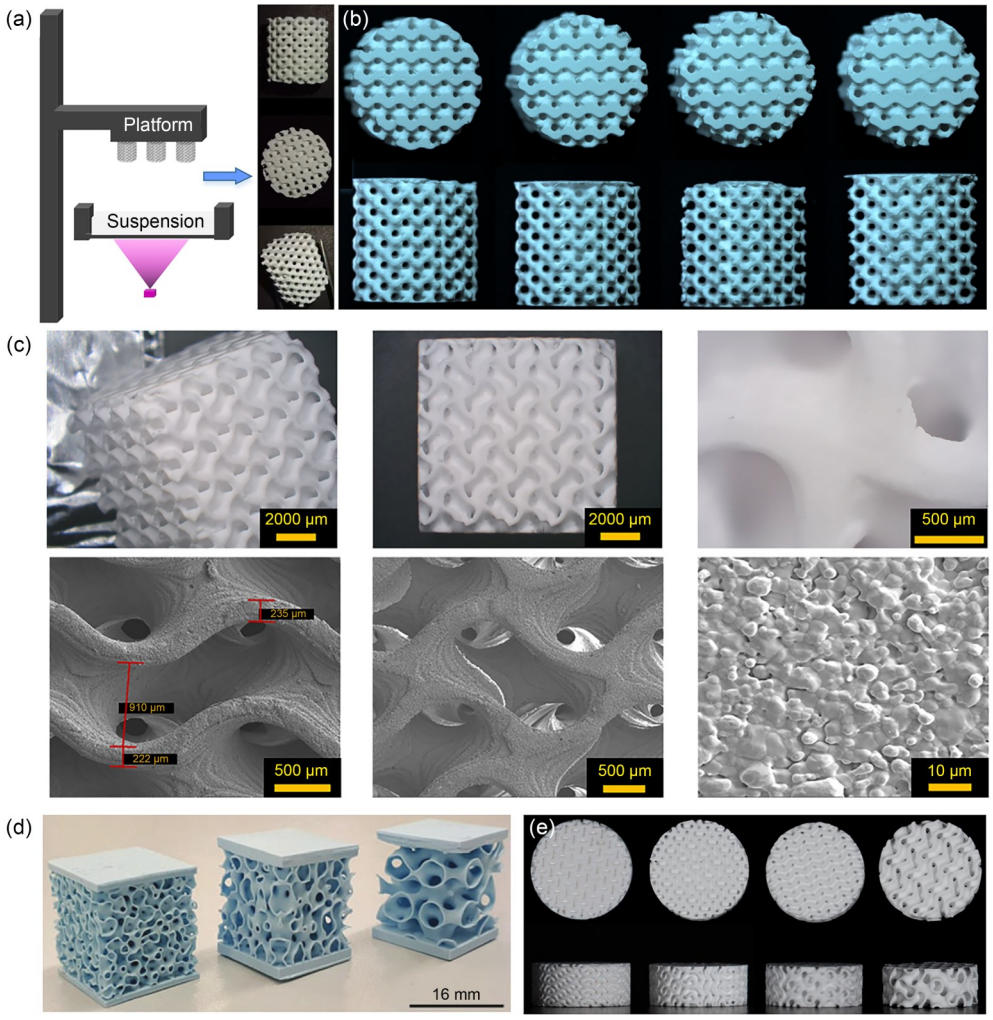

Fig. 13 Fabrication of ceramic-based TPMS structures using DLP. (a) Flow diagram of gyroid structural bioceramic green bodies fabricated using DLP (reproduced from [190], Copyright 2021, with permission from Elsevier). (b) Macrostructure of printed TPMS scaffolds with different gradient structures (reproduced from [37], Copyright 2023, with permission from Elsevier). (c) Gyroid design obtained for the ceramic scaffolds and SEM micrographs of structural details (reproduced from [186], Copyright 2023, with permission from the authors, licensed under CC BY-NC-ND). (d) Fabricated TPMS derivative ceramic structures (reproduced from [185], Copyright 2023, with permission from the authors, licensed under CC BY). (e) Digital photos of TPMS bone scaffold with various porosities (reproduced from [191], Copyright 2024, with permission from the authors, licensed under CC BY-NC). SEM: scanning electron microscope

fabricated HA ceramics with TPMS structures using DLP (Fig. 13a), enhanced by doping akermanite to better tailor the porosity, bioactivity, and mechanical strength.

In addition to HA, other bioceramics are used for DLP of TPMS-based bone implants and extensive research has been conducted to investigate their applications. For example, Lu et al. [192] fabricated ZnO ceramics with gyroid and Schwartz P TPMS structures using DLP. The gyroid-structured ZnO ceramic exhibited a compressive strength of approximately 6.87 MPa with 55% porosity, outperforming the Schwartz P structure, which showed 4.02 MPa. Jiao et al. [193] fabricated bone scaffolds with variable irregularity and porosity using ceramic DLP with 20% (mass fraction) HA-doped zirconia. The scaffolds mimicking the cancellous bone structure demonstrated enhanced mechanical and biocompatibility properties. Shao et al. [194] investigated ZrO_2/CSi–Mg*x* scaffolds fabricated via DLP by combining Mg-doped calcium silicate (CSi–Mg) with ZrO_2 to enhance their biocompatibility and mechanical properties. The incorporation of CSi–Mg significantly strengthened the scaffolds after sintering, with the ZrO_2/CSi–Mg10 scaffolds featuring TPMS showing compression strengths exceeding 92 MPa, and a strength of 63 MPa even after prolonged immersion. Shen et al. [195] focused on tailoring the pore architectures of Mg-doped scaffolds using DLP to achieve fully interconnected networks and TPMSs resembling cancellous bone. The sheet-TPMS geometries exhibited higher initial compressive strength and higher Mg-ion release rates than other TPMS structures in vitro. Zhu et al. [191] fabricated four TPMS configurations (Fig. 13e) with β-TCP bioceramic

via DLP and studied the substantial potential of TPMS scaffolds for promoting bone regeneration within mandibular defects. Duque-Uribe et al. [196] fabricated alumina (Al_2O_3) scaffolds using ceramic DLP and a suspension of Al_2O_3 particles in a photopolymerizable resin. Scaffolds with gyroid and Schwartz P geometries were successfully printed and characterized morphologically and mechanically pre- and postsintering. Li et al. [197] fabricated Mg/Sr co-doped wollastonite bioceramic (MS−CSi) scaffolds with gyroid, cylindrical, and cubic pore geometries fabricated using DLP and investigated their impact on osteogenesis and angiogenesis through in vitro and in vivo experiments. Vijayavenkataraman et al. [198] explored porous bone implant designs based on TPMS and fabricated them using Al_2O_3 via DLP. This research demonstrated the feasibility of 3D printing TPMS-based structures in ceramics, highlighting the potential to match the compressive modulus of native bone and mitigate stress shielding effects in bone implant applications.

4 Biological performance of TPMS-based bone implants

The biological performance evaluation of TPMS-based bone implants encompasses several critical aspects. First, their mechanical properties are rigorously assessed through experimental testing and simulation to ensure that they match the structural integrity required for load-bearing applications. Second, permeability studies combining experimental measurements and computational simulations are conducted to investigate how the intricate TPMS structures facilitate nutrient diffusion and waste removal essential for tissue viability. Third, biocompatibility is evaluated through comprehensive in vitro and in vivo experiments to investigate how well these implants interact with biological systems, focusing on aspects like cell adhesion, proliferation, and inflammatory responses. These investigations validate TPMS-based bone implants as robust, biocompatible solutions for enhancing bone regeneration and integration in clinical settings.

4.1 Mechanical properties

The mechanical performance of TPMS-based implants is crucially evaluated using parameters like compressive strength, modulus of elasticity, and fatigue resistance (Fig. 14b) [199, 200]. Compressive strength is a key mechanical property of TPMS-based implants, reflecting their ability to withstand compressive forces in weight-bearing bones [36, 125]. Experimental studies involve subjecting these implants to compression tests to determine the maximum load they can bear before failure. The intricate porous architecture of TPMS provides structural support while maintaining sufficient porosity for biological integration, resulting in compressive strengths comparable to those of cancellous bone. The modulus of elasticity, also known as Young's modulus, measures the stiffness of TPMS-based implants [93, 115]. This property is critical as it determines how much an implant deforms under applied stress. TPMS structures, with their open-cell design and variable pore sizes, can be tailored to achieve moduli that closely match those of natural bone, thereby minimizing stress shielding effects and promoting load transfer between the implant and surrounding bone tissue. In addition to efficiently adjusting the porosity to tailor the mechanical properties of TPMS structures, various gradient structures have been used to create porous bone implants that more closely match the characteristics of natural bone [38, 40, 200, 201]. These gradient designs allow for a more seamless integration with the native bone, thereby enhancing the functionality and effectiveness of the implant. By mimicking the natural gradation found in bone tissue, these TPMS-based implants can offer improved mechanical compatibility and biological performance, ultimately leading to better outcomes in bone regeneration and repair.

Furthermore, fatigue resistance was evaluated to examine the long-term durability of TPMS-based implants under cyclic loading conditions [106, 118, 133]. Fatigue tests simulate the repetitive stresses that implants may experience during daily activities to ensure that they can withstand mechanical wear over extended periods without structural failure. The interconnected network of pores within TPMS structures enhances their fatigue resistance by evenly distributing stress throughout the implant, thereby reducing the likelihood of crack propagation and failure. Speirs et al. [133] investigated the compression fatigue behavior of several TPMS scaffolds and found that TPMS offers superior static mechanical properties and fatigue resistance compared to conventional structures. Yang et al. [118] examined the compression–compression fatigue behavior of the gyroid cellular structures and found that cyclic ratcheting and fatigue damage contribute to failure, typically resulting in nearly 45° fracture bands. The fatigue ratio was increased after sandblasting, which enhanced the fatigue resistance by removing adhered powder particles, inducing compressive residual stress, and creating a nanocrystalline zone, thus outperforming many other lattice structures. Tilton et al. [106] revealed new insights into the fatigue performance of Ti-6Al-4V scaffolds fabricated using TPMS. They found that the Schoen-IWP scaffolds exhibited a significantly higher fatigue life than the primitive scaffolds at similar porosity and applied stress amplitude, although the primitive scaffolds better mimicked the compressive mechanical properties of the trabecular bone. These findings are crucial for the spatial microarchitectural design of load-bearing orthopedic implants.

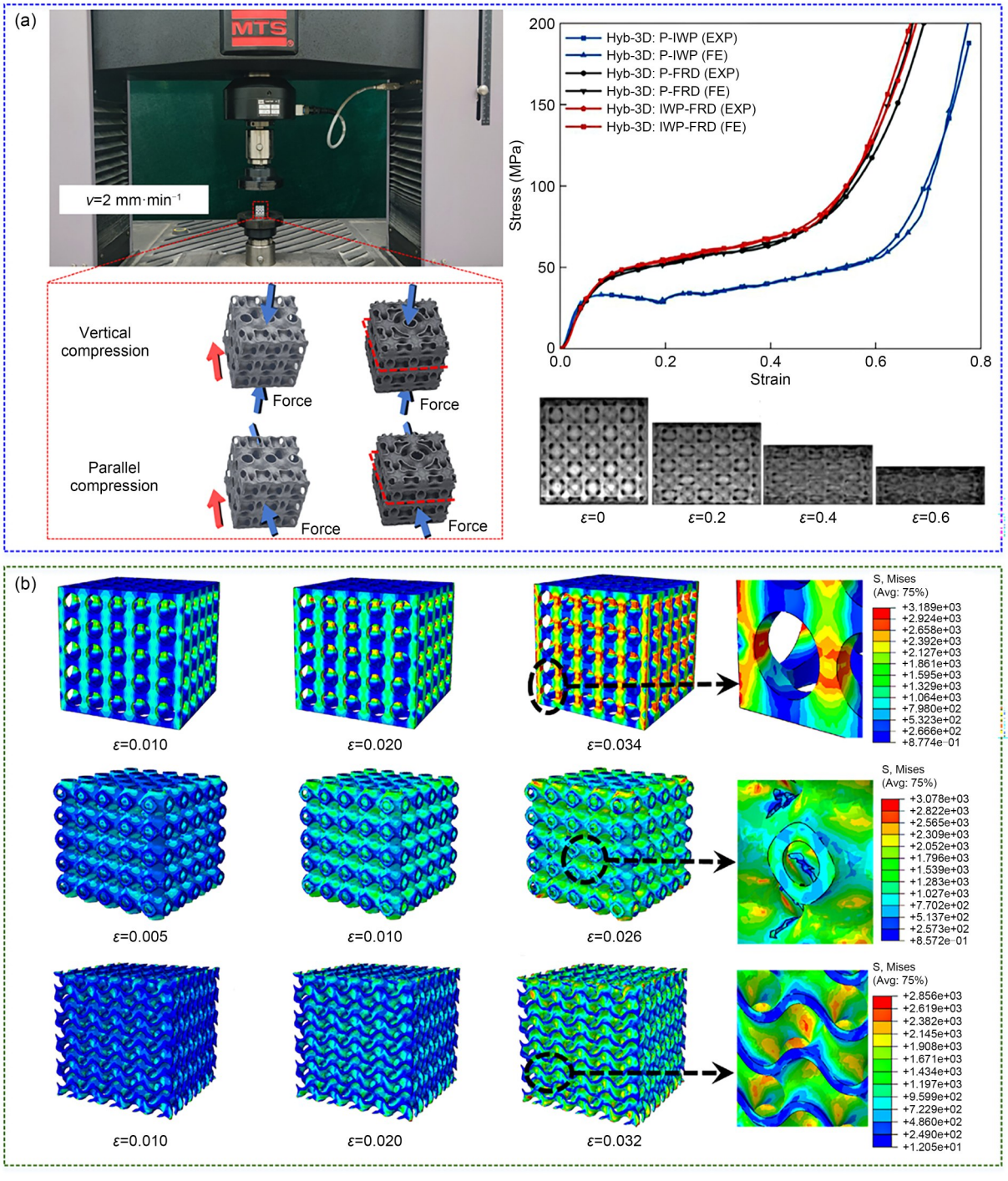

Fig. 14 Investigation of the mechanical properties of TPMS-based scaffolds. (a) Experimental method (reproduced from [93], Copyright 2024, with permission from Elsevier). (b) Numerical method (reproduced from [199], Copyright 2023, with permission from Elsevier)

Therefore, the mechanical properties of TPMS-based bone implants are carefully engineered to replicate and enhance the biomechanical functions of natural bone. Moreover, TPMS-based implants offer promising solutions for improving the longevity and performance of orthopedic implants in clinical practice by optimizing compressive strength, modulus of elasticity, and fatigue resistance through advanced fabrication techniques and material selection.

4.2 Permeability

Permeability is another critical characteristic of TPMS-based bone implants that influences their ability to facilitate

nutrient transportation, waste removal, and cell migration within the porous structure of the implant [202]. TPMS structures, inspired by natural bone's trabecular architecture, are designed to optimize permeability while maintaining mechanical integrity. The intricate network of interconnected pores in TPMS implants allows for efficient fluid flow and gas exchange, which are crucial for cellular activities, such as proliferation, differentiation, and tissue regeneration [49, 50].

Numerous experimental studies combined with computational simulations have been conducted to comprehensively examine the permeability of TPMS-based implants. Permeability experiments involve measuring the flow of fluids through the implant under controlled conditions and providing quantitative data on how well fluids can penetrate and permeate through the scaffold's porous network. The constant head permeability test setup is commonly used to experimentally measure the permeability of scaffolds, with the samples tightly fixed using two clamps between two reservoirs [43]. Computational fluid dynamics (CFD) simulations complement these experiments by predicting fluid flow patterns and pressure gradients within the TPMS structure, providing insights into the transport properties of implants under varying physiological conditions [10, 63, 203–207] (Fig. 15).

The permeability of TPMS-based implants is influenced by several factors, including the pore size, shape, interconnectivity, and overall porosity [208]. Larger pores and interconnected channels enhance permeability by reducing the flow resistance, thereby allowing for better nutrient diffusion and waste removal. However, the permeability must also be optimized while maintaining sufficient mechanical strength and structural integrity to support the surrounding tissue and withstand physiological loads. Therefore, the permeability of TPMS-based bone implants plays a crucial role in their biological performance by facilitating fluid exchange and nutrient transport, which are crucial for cellular activities and tissue regeneration [116, 204]. Recent advances in experimental techniques and computational modeling have continuously refined our understanding of how TPMS structures can be tailored to maximize permeability while satisfying the mechanical and biological requirements for successful orthopedic applications.

4.3 Biocompatibility

Biocompatibility is a very important criterion for the successful application of TPMS-based bone implants, which ensures that the implants interact favorably with biological systems [41, 200]. To comprehensively evaluate biocompatibility, in vitro and in vivo studies have been conducted, focusing on key aspects like cell adhesion, proliferation, and inflammatory responses [195, 209].

In vitro studies are typically the first step in assessing the biocompatibility of TPMS-based bone implants. These studies involve culturing various types of cells, such as osteoblasts or BMSCs, on the implant surfaces to observe cell adhesion, spreading, and proliferation. Successful cell adhesion indicates a surface that supports cellular attachment, which is a critical factor for subsequent tissue integration. Ma et al. [41] conducted cell–culture experiments to investigate the effects of pore size and scaffold porosity on cell growth. The fabricated TPMS scaffolds exhibited good biocompatibility, and the surface area and permeability can affect the degrees of cell adhesion and proliferation. Jin et al. [43] conducted in vitro studies by infiltrating the soft gelatin methacryloyl (GelMA) hydrogel matrix into the pores of the fabricated scaffolds to demonstrate its biocompatibility. The results provide insights into the design and application of porous scaffolds in bone implants. Xu et al. [200] conducted an in vitro biomineralization and biological testing and found that the TPMS scaffolds showed excellent calcium-phosphorus formation induction and biocompatibility (Fig. 16a).

In vivo studies provide a more comprehensive assessment of biocompatibility by implanting TPMS-based scaffolds into animal models [186, 197]. These studies examine the overall body response to implants, focusing on tissue integration, inflammatory reactions, and bone regeneration [187, 210]. Histological analyses are conducted to evaluate the extent of new bone formation, vascularization, and the integration of the implant with surrounding tissue. These analyses often include staining techniques to identify specific cell types and the deposition of a new bone matrix. Shen et al. [195] analyzed rabbit experiments in vivo to show that although bone regeneration is delayed in sheet-TPMS pore geometries, diamond and gyroid pore scaffolds significantly enhance early-stage osteogenesis and achieve uniform bone tissue formation by seven weeks. This finding highlights the effectiveness of diamond and gyroid architectures in accelerating bone regeneration and improving scaffold performance in bone defect repair. Khan et al. [211] conducted an in vivo study to evaluate the integration of gyroid-based Ti6Al-4V implants over six weeks using a rabbit tibia model (Fig. 16b). Histopathological examination revealed superior osteointegration in the gyroid structures, as evidenced by neovascularization, in-bone growth, and the presence of a Haversian system. Zhao et al. [44] conducted an in vivo study on Zn-based bone implants and demonstrated expedited bone ingrowth and regeneration through the sustained release of divalent metal cations. These implants significantly enhanced osteogenesis, immunoregulation, angiogenesis, and anti-infective activity, highlighting their promising potential for clinical translation in repairing load-bearing bone defects. Wang et al. [212] conducted in vivo tests on Zn–2Mg alloy scaffolds to demonstrate

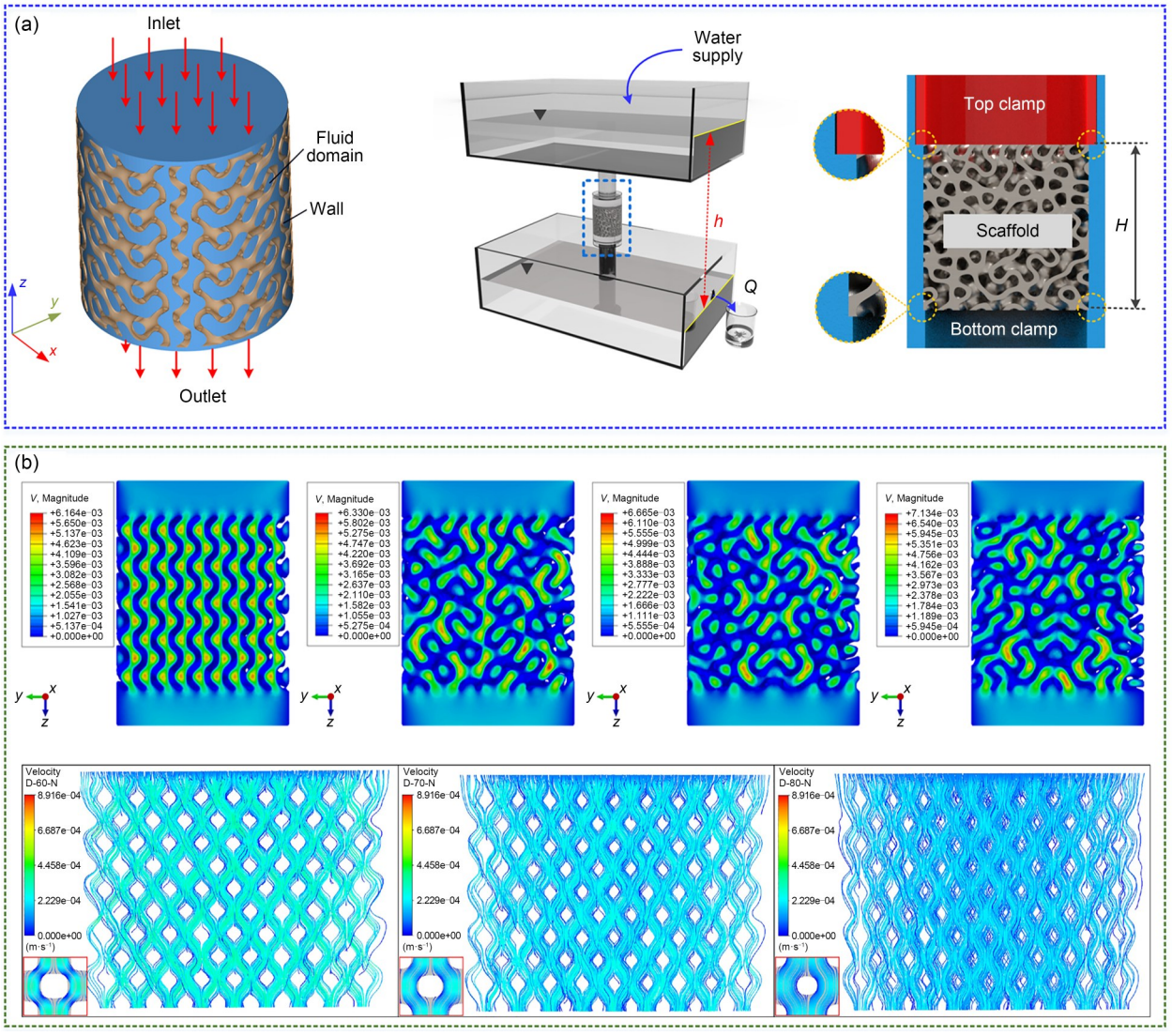

Fig. 15 Investigation of the permeability of TPMS-based scaffolds. (a) Experimental setup of the constant head method and boundary conditions for the CFD analysis (reproduced from [43], Copyright 2022, with permission from Elsevier). (b) Results from CFD analysis (reproduced from [43] (Copyright 2022, with permission from Elsevier) and [207] (Copyright 2023, with permission from IPEM))

their satisfactory biocompatibility and osteogenic ability. They found that scaffolds with lower porosities and smaller unit sizes exhibited superior osteogenesis because of their optimal pore size and larger surface area. These findings indicate that the biodegradable performance of these scaffolds can be precisely regulated through their structural design, making them highly effective for treating bone defects.

Overall, the biocompatibility of TPMS-based bone implants has been extensively evaluated via in vitro and in vivo studies. These studies focused on essential factors like cell adhesion, proliferation, and inflammatory responses to ensure that implants interact positively with biological systems. The primary objective is to develop implants that support tissue integration and regeneration to provide a reliable solution for bone repair and regeneration.

5 Conclusions and future perspectives

This review presented a comprehensive overview of the current state-of-the-art research on bone implants with TPMS architectures, focusing on their design, fabrication, and biological performance. The integration of TPMS structures into bone implants has shown significant promise because of their ability to closely mimic the intricate geometry and mechanical properties of natural bone. However, there are several key challenges that must be addressed to fully exploit the potential of TPMS-based bone implants in clinical applications.

The design of TPMS-based bone implants offers a unique advantage in terms of mechanical properties that can be fine-tuned to match those of natural bone. The TPMS

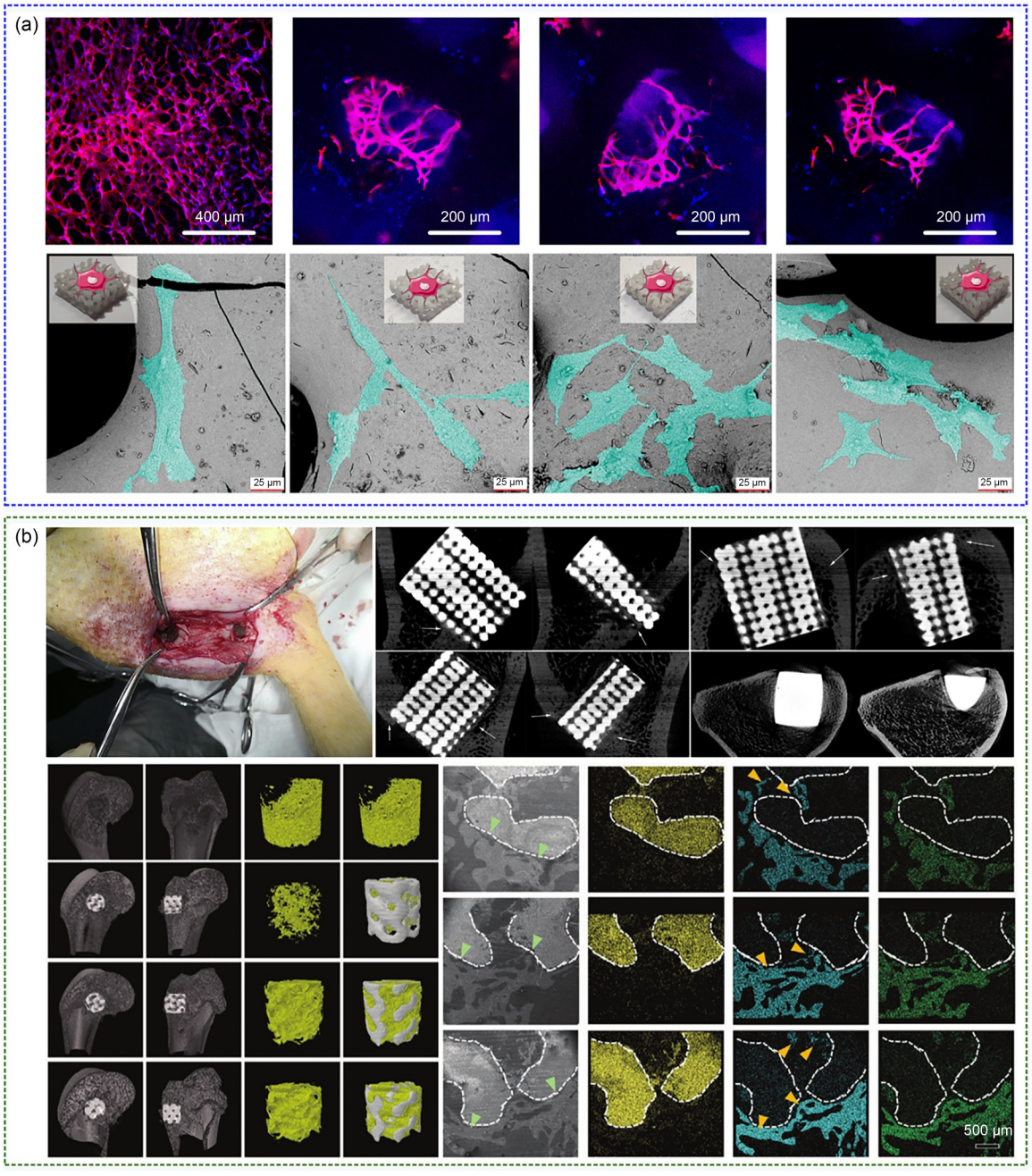

Fig. 16 Studies on the biocompatibility of TPMS-based scaffolds. (a) In vitro experiment (reproduced from [43] (Copyright 2022, with permission from Elsevier) and [200] (Copyright 2024, with permission from Elsevier)). (b) In vivo experiment (reproduced from [210] (Copyright 2019, with permission from the authors, licensed under CC BY-NC-ND) and [44] (Copyright 2023, with permission from Wiley-VCH GmbH))

structures, such as gyroid, diamond, and Schoen's IWP, provide a balance between strength and porosity, which is essential for load-bearing applications and for facilitating bone ingrowth. However, optimizing these designs requires further exploration of the specific mechanical and biological requirements of different types of bone defects and patient-specific conditions. The existing gradient, hierarchical, and hybrid designs are often based on idealized and generalized models obtained from medical imaging, including finite element analysis of the post-design medical mechanical properties. Due to the complex properties, loads, and boundary conditions of the corresponding materials in the human body, it is difficult to evaluate them with high accuracy in the design stage due to the limitations of computer operations and medical detection methods. In other words, we can only set one or a few goals for optimization, and it is difficult to achieve a quantitative analysis of the customized design and subsequent interface response

for existing patients. In particular, for the local matching problem of bone defects and joint replacements, it is necessary to consider the integration of biomechanics and mechanobiology with existing bone segments to solve stress shielding and implant settlement potential. Future research should focus on developing advanced computational models and simulation techniques to predict the performance of these implants more accurately under physiological conditions.

The fabrication of TPMS-based bone implants has been revolutionized by advancements in AM technologies, especially LPBF and DLP. These methods enable the precise creation of complex TPMS structures with high resolution and reproducibility. Despite these advancements, there are still challenges, such as the scalability of production, material limitations, and the integration of multiple materials to enhance the functional properties of implants. The existing AM accuracy is insufficient to support our design exploration of TPMS bone implants. There are various manufacturing defects at scales below 100 μm, and some surface modification methods are also difficult to meet the requirements of this complex structure. The differences between design and manufacturing greatly reduce the original design goals, and the ideal effects could be observed in subsequent in vitro and in vivo experiments. Future work should aim at refining these fabrication techniques to improve their efficiency, cost-effectiveness, and ability to produce multimaterial implants with integrated functionalities.

In terms of biological performance, TPMS-based implants have exhibited enhanced osteogenesis, vascularization, and integration with host bone tissue. The interconnected porous networks of the TPMS structures facilitate nutrient and waste exchange, promoting cell proliferation and differentiation. This can be achieved by adjusting the volume fraction and inner-to-outer pore volume ratio, which respectively influence the scaffold's elastic modulus and permeability. By fine-tuning these parameters, implants that provide the necessary mechanical support can be created while also ensuring effective mass transport, which is crucial for the success of the implant in vivo. As discussed in this review, previous studies have shown promising results in terms of bone regeneration and implant stability. However, the long-term biological effects and potential complications related to the degradation products of these implants require further investigation. Future research should include long-term in vivo experiments and clinical trials to comprehensively evaluate the safety and efficacy of TPMS-based implants.

In addition to the discussed aspects, future developments of TPMS-based bone implants should explore the integration of advanced functionalities, such as metamaterials. These materials can offer unique properties not found in traditional materials, such as negative Poisson's ratio or tunable acoustic properties, which could enhance the overall performance and adaptability of bone implants. Incorporating metamaterials into TPMS designs can improve biomechanical compatibility and promote more effective load transfer during bone regeneration. Furthermore, the use of biodegradable materials is a promising area for future research. These materials can gradually transfer the load to the regenerating bone while maintaining mechanical integrity, thereby promoting natural healing processes. Advancements in material science have led to the development of biodegradable alloys and composites that balance degradation rates with mechanical strength, thereby optimizing long-term implant performance.

In conclusion, although significant progress has been made in the design, fabrication, and biological performance of TPMS-based bone implants, future research should focus on integrating metamaterials, advancing biodegradable materials, and leveraging personalized medicine approaches. These strategies can revolutionize the field of orthopedic implantology by providing safer, more effective, and personalized solutions for bone defect repair and regeneration.

Acknowledgements This research was funded by the National Natural Science Foundation of China (No. 52275343), the Natural Science Foundation of Zhejiang Province (No. LY23E050003), Ningbo Youth Science and Technology Innovation Leading Talent Project (No. 2023QL021), and Smart Medicine and Engineering Interdisciplinary Innovation Project of Ningbo University (No. ZHYG001).

Author contributions JHL: conceptualization, investigation, data analysis, writing—original draft, and writing—review & editing. HTF: investigation, data analysis, writing—original draft, and resources. LCH: investigation, data analysis, supervision, and resources. JKD: methodology, supervision, resources, and project administration. YH: conceptualization, methodology, supervision, resources, and project administration. YAJ: conceptualization, methodology, supervision, writing—original draft, project administration, and funding acquisition.

Declarations

Conflict of interest YH is an associate editor for *Bio-Design and Manufacturing* and was not involved in the editorial review or the decision to publish this article. The authors declare that they have no conflict of interest.

Ethical approval This study does not contain any studies with human or animal subjects performed by any of the authors.

References

1. Puleo DA, Nanci A (1999) Understanding and controlling the bone-implant interface. Biomaterials 20(23–24):2311–2321. https://doi.org/10.1016/s0142-9612(99)00160-x
2. Yang YW, He CX, Dianyu E et al (2020) Mg bone implant: features, developments and perspectives. Mater Des 185:108259. https://doi.org/10.1016/j.matdes.2019.108259
3. Verma RP (2020) Titanium based biomaterial for bone implants: a mini review. Mater Today Proc 26:3148–3151. https://doi.org/10.1016/j.matpr.2020.02.649

4. Shah FA, Thomsen P, Palmquist A (2019) Osseointegration and current interpretations of the bone-implant interface. Acta Biomater 84:1–15. https://doi.org/10.1016/j.actbio.2018.11.018
5. Balla VK, Bodhak S, Bose S et al (2010) Porous tantalum structures for bone implants: fabrication, mechanical and in vitro biological properties. Acta Biomater 6(8):3349–3359. https://doi.org/10.1016/j.actbio.2010.01.046
6. Feng JW, Fu JZ, Yao XH et al (2022) Triply periodic minimal surface (TPMS) porous structures: from multi-scale design, precise additive manufacturing to multidisciplinary applications. Int J Extrem Manuf 4(2):022001. https://doi.org/10.1088/2631-7990/ac5be6
7. Poltue T, Karuna C, Khrueaduangkham S et al (2021) Design exploration of 3D-printed triply periodic minimal surface scaffolds for bone implants. Int J Mech Sci 211:106762. https://doi.org/10.1016/j.ijmecsci.2021.106762
8. Dong ZF, Zhao X (2021) Application of TPMS structure in bone regeneration. Eng Regen 2:154–162. https://doi.org/10.1016/j.engreg.2021.09.004
9. Verma R, Kumar J, Singh NK et al (2022) Design and analysis of biomedical scaffolds using TPMS-based porous structures inspired from additive manufacturing. Coatings 12(6):839. https://doi.org/10.3390/coatings12060839
10. Li ZT, Chen ZB, Chen XB et al (2024) Design and evaluation of TPMS-inspired 3D-printed scaffolds for bone tissue engineering: enabling tailored mechanical and mass transport properties. Compos Struct 327:117638. https://doi.org/10.1016/j.compstruct.2023.117638
11. Song KL, Wang ZH, Lan J et al (2021) Porous structure design and mechanical behavior analysis based on TPMS for customized root analogue implant. J Mech Behav Biomed Mater 115: 104222. https://doi.org/10.1016/j.jmbbm.2020.104222
12. Parthasarathy J, Starly B, Raman S (2011) A design for the additive manufacture of functionally graded porous structures with tailored mechanical properties for biomedical applications. J Manuf Process 13(2):160–170. https://doi.org/10.1016/j.jmapro.2011.01.004
13. Egan PF, Ferguson SJ, Shea K (2017) Design of hierarchical three-dimensional printed scaffolds considering mechanical and biological factors for bone tissue engineering. J Mech Des 139(6): 061401. https://doi.org/10.1115/1.4036396
14. Naghavi SA, Tamaddon M, Garcia-Souto P et al (2023) A novel hybrid design and modelling of a customised graded Ti-6Al-4V porous hip implant to reduce stress-shielding: an experimental and numerical analysis. Front Bioeng Biotechnol 11:1092361. https://doi.org/10.3389/fbioe.2023.1092361
15. Wang XJ, Xu SQ, Zhou SW et al (2016) Topological design and additive manufacturing of porous metals for bone scaffolds and orthopaedic implants: a review. Biomaterials 83:127–141. https://doi.org/10.1016/j.biomaterials.2016.01.012
16. Catchpole-Smith S, Sélo RRJ, Davis AW et al (2019) Thermal conductivity of TPMS lattice structures manufactured via laser powder bed fusion. Addit Manuf 30:100846. https://doi.org/10.1016/j.addma.2019.100846
17. Yuan L, Ding SL, Wen CE (2019) Additive manufacturing technology for porous metal implant applications and triple minimal surface structures: a review. Bioact Mater 4:56–70. https://doi.org/10.1016/j.bioactmat.2018.12.003
18. Ge JG, Huang Q, Wang Y et al (2023) Microstructural optimization and mechanical enhancement of SLM Ti6Al4V TPMS scaffolds through vacuum annealing treatment. J Alloys Compd 934:167524. https://doi.org/10.1016/j.jallcom.2022.167524
19. Lal Lazar PJ, Subramanian J, Natarajan E et al (2023) Anisotropic structure-property relations of FDM printed short glass fiber reinforced polyamide TPMS structures under quasi-static compression. J Mater Res Technol 24:9562–9579. https://doi.org/10.1016/j.jmrt.2023.05.167
20. Mishra AK, Chavan H, Kumar A (2021) Effect of material variation on the uniaxial compression behavior of FDM manufactured polymeric TPMS lattice materials. Mater Today Proc 46: 7752–7759. https://doi.org/10.1016/j.matpr.2021.02.276
21. Zheng XX, Duan F, Song ZY et al (2022) A TMPS-designed personalized mandibular scaffolds with optimized SLA parameters and mechanical properties. Front Mater 9:966031. https://doi.org/10.3389/fmats.2022.966031
22. Temiz A (2024) The effect of build orientation on the mechanical properties of a variety of polymer AM-created triply periodic minimal surface structures. J Braz Soc Mech Sci Eng 46(3):121. https://doi.org/10.1007/s40430-024-04709-0
23. Rueschhoff L, Costakis W, Michie M et al (2016) Additive manufacturing of dense ceramic parts via direct ink writing of aqueous alumina suspensions. Int J Appl Ceram Technol 13(5):821–830. https://doi.org/10.1111/ijac.12557
24. Yang CG, Wu WC, Fu Z et al (2023) Preparation and thermal insulation properties of TPMS 3Y-TZP ceramics using DLP 3D printing technology. J Mater Sci 58(29):11992–12007. https://doi.org/10.1007/s10853-023-08749-0
25. Liu K, Zhang ZJ, Sun HJ et al (2023) Fabrication and mechanical properties of triply period minimal surface porous alumina ceramics based on digital light processing 3D printing technology. Int J Adv Manuf Technol (early access). https://doi.org/10.1007/s00170-023-11164-z
26. Pugliese R, Graziosi S (2023) Biomimetic scaffolds using triply periodic minimal surface-based porous structures for biomedical applications. SLAS Technol 28(3):165–182. https://doi.org/10.1016/j.slast.2023.04.004
27. Li YF, Liu HW, Wang C et al (2023) 3D printing titanium grid scaffold facilitates osteogenesis in mandibular segmental defects. npj Regen Med 8(1):38. https://doi.org/10.1038/s41536-023-00308-0
28. Motomura G, Mashima N, Imai H et al (2022) Effects of porous tantalum on periprosthetic bone remodeling around metaphyseal filling femoral stem: a multicenter, prospective, randomized controlled study. Sci Rep 12(1):914. https://doi.org/10.1038/s41598-022-04936-2
29. Park JW, Park H, Kim JH et al (2022) Fabrication of a lattice structure with periodic open pores through three-dimensional printing for bone ingrowth. Sci Rep 12(1):17223. https://doi.org/10.1038/s41598-022-22292-z
30. Zhou XY, Jin Y, Du JK (2020) Functionally graded scaffolds with programmable pore size distribution based on triply periodic minimal surface fabricated by selective laser melting. Materials 13(21):5046. https://doi.org/10.3390/ma13215046
31. Zhang JF, Chen XH, Sun YX et al (2022) Design of a biomimetic graded TPMS scaffold with quantitatively adjustable pore size. Mater Des 218:110665. https://doi.org/10.1016/j.matdes.2022.110665
32. Jin Y, Kong HY, Zhou XY et al (2020) Design and characterization of sheet-based gyroid porous structures with bioinspired functional gradients. Materials 13(17):3844. https://doi.org/10.3390/ma13173844
33. Zhang L, Hu ZH, Wang MY et al (2021) Hierarchical sheet triply periodic minimal surface lattices: design, geometric and mechanical performance. Mater Des 209:109931.

https://doi.org/10.1016/j.matdes.2021.109931
34. Al-Ketan O, Abu Al-Rub RK (2021) MSLattice: a free software for generating uniform and graded lattices based on triply periodic minimal surfaces. Mater Des Process Commun 3(6):e205. https://doi.org/10.1002/mdp2.205
35. Gao TY, Liu K, Wang XX et al (2022) Elastic mechanical property hybridization of configuration-varying TPMS with geometric continuity. Mater Des 221:110995. https://doi.org/10.1016/j.matdes.2022.110995
36. Li M, Jiang JW, Liu WB et al (2023) Bioadaptable bioactive glass-β-tricalcium phosphate scaffolds with TPMS-gyroid structure by stereolithography for bone regeneration. J Mater Sci Technol 155:54–65. https://doi.org/10.1016/j.jmst.2023.01.025
37. Deng ZL, Pan MZ, Hua SB et al (2023) Mechanical and degradation properties of triply periodic minimal surface (TPMS) hydroxyapatite & akermanite scaffolds with functional gradient structure. Ceram Int 49(12):20808–20816. https://doi.org/10.1016/j.ceramint.2023.03.213
38. Kanwar S, Vijayavenkataraman S (2022) 3D printable bone-mimicking functionally gradient stochastic scaffolds for tissue engineering and bone implant applications. Mater Des 223: 111199. https://doi.org/10.1016/j.matdes.2022.111199
39. Cao YX, Lai SY, Wu WY et al (2023) Design and mechanical evaluation of additively-manufactured graded TPMS lattices with biodegradable polymer composites. J Mater Res Technol 23:2868–2880. https://doi.org/10.1016/j.jmrt.2023.01.221
40. Liao B, Xia RF, Li W et al (2021) 3D-printed Ti6Al4V scaffolds with graded triply periodic minimal surface structure for bone tissue engineering. J Mater Eng Perform 30(7):4993–5004. https://doi.org/10.1007/s11665-021-05580-z
41. Ma S, Tang Q, Han XX et al (2020) Manufacturability, mechanical properties, mass-transport properties and biocompatibility of triply periodic minimal surface (TPMS) porous scaffolds fabricated by selective laser melting. Mater Des 195:109034. https://doi.org/10.1016/j.matdes.2020.109034
42. Li ZT, Chen ZB, Chen XB et al (2024) Multi-objective optimization for designing porous scaffolds with controllable mechanics and permeability: a case study on triply periodic minimal surface scaffolds. Compos Struct 333:117923. https://doi.org/10.1016/j.compstruct.2024.117923
43. Jin Y, Zou SJ, Pan BC et al (2022) Biomechanical properties of cylindrical and twisted triply periodic minimal surface scaffolds fabricated by laser powder bed fusion. Addit Manuf 56:102899. https://doi.org/10.1016/j.addma.2022.102899
44. Zhao DL, Yu KD, Sun TF et al (2023) Material–structure–function integrated additive manufacturing of degradable metallic bone implants for load-bearing applications. Adv Funct Mater 33(16):2213128. https://doi.org/10.1002/adfm.202213128
45. Yang Y, Xu T, Bei HP et al (2022) Gaussian curvature-driven direction of cell fate toward osteogenesis with triply periodic minimal surface scaffolds. Proc Natl Acad Sci USA 119(41): e2206684119. https://doi.org/10.1073/pnas.2206684119
46. Negrescu AM, Necula MG et al (2020) In vitro and in vivo biological performance of Mg-based bone implants. Rev Biol Biomed Sci 3(1):11–41
47. Habibovic P, Li JP, van der Valk CM et al (2005) Biological performance of uncoated and octacalcium phosphate-coated Ti6Al4V. Biomaterials 26(1):23–36. https://doi.org/10.1016/j.biomaterials.2004.02.026
48. Hannink G, Arts JJC (2011) Bioresorbability, porosity and mechanical strength of bone substitutes: what is optimal for bone regeneration? Injury 42:S22–S25. https://doi.org/10.1016/j.injury.2011.06.008
49. Castro AG, Pires T, Santos JE et al (2019) Permeability versus design in TPMS scaffolds. Materials 12(8):1313. https://doi.org/10.3390/ma12081313
50. Santos J, Pires T, Gouveia BP et al (2020) On the permeability of TPMS scaffolds. J Mech Behav Biomed Mater 110:103932. https://doi.org/10.1016/j.jmbbm.2020.103932
51. Liu K, Zhou Q, Zhang XQ et al (2023) Morphologies, mechanical and in vitro behaviors of DLP-based 3D printed HA scaffolds with different structural configurations. RSC Adv 13(30): 20830–20838. https://doi.org/10.1039/d3ra03080f
52. Yoo DJ (2011) Porous scaffold design using the distance field and triply periodic minimal surface models. Biomaterials 32(31): 7741–7754. https://doi.org/10.1016/j.biomaterials.2011.07.019
53. Kapfer SC, Hyde ST, Mecke K et al (2011) Minimal surface scaffold designs for tissue engineering. Biomaterials 32(29): 6875–6882. https://doi.org/10.1016/j.biomaterials.2011.06.012
54. Yoo DJ (2011) Computer-aided porous scaffold design for tissue engineering using triply periodic minimal surfaces. Int J Precis Eng Manuf 12(1):61–71. https://doi.org/10.1007/s12541-011-0008-9
55. Yoo DJ (2012) New paradigms in internal architecture design and freeform fabrication of tissue engineering porous scaffolds. Med Eng Phys 34(6):762–776. https://doi.org/10.1016/j.medengphy.2012.05.008
56. Zhu X, Chen F, Cao H et al (2023) Design and fused deposition modeling of triply periodic minimal surface scaffolds with channels and hydrogel for breast reconstruction. Int J Bioprint 9(2):685. https://doi.org/10.18063/ijb.685
57. Fan XJ, Tang Q, Feng QX et al (2021) Design, mechanical properties and energy absorption capability of graded-thickness triply periodic minimal surface structures fabricated by selective laser melting. Int J Mech Sci 204:106586. https://doi.org/10.1016/j.ijmecsci.2021.106586
58. Al-Ketan O, Rowshan R, Abu Al-Rub RK (2018) Topology-mechanical property relationship of 3D printed strut, skeletal, and sheet based periodic metallic cellular materials. Addit Manuf 19:167–183. https://doi.org/10.1016/j.addma.2017.12.006
59. Zhou HL, Zhao M, Ma ZB et al (2020) Sheet and network based functionally graded lattice structures manufactured by selective laser melting: design, mechanical properties, and simulation. Int J Mech Sci 175:105480. https://doi.org/10.1016/j.ijmecsci.2020.105480
60. Cai ZZ, Liu ZH, Hu XD et al (2019) The effect of porosity on the mechanical properties of 3D-printed triply periodic minimal surface (TPMS) bioscaffold. Bio-Des Manuf 2(4):242–255. https://doi.org/10.1007/s42242-019-00054-7
61. Taniguchi N, Fujibayashi S, Takemoto M et al (2016) Effect of pore size on bone ingrowth into porous titanium implants fabricated by additive manufacturing: an in vivo experiment. Mater Sci Eng C 59:690–701. https://doi.org/10.1016/j.msec.2015.10.069
62. Van Bael S, Chai YC, Truscello S et al (2012) The effect of pore geometry on the in vitro biological behavior of human periosteum-derived cells seeded on selective laser-melted Ti6Al4V bone scaffolds. Acta Biomater 8(7):2824–2834. https://doi.org/10.1016/j.actbio.2012.04.001
63. Montazerian H, Davoodi E, Asadi-Eydivand M et al (2017)

Porous scaffold internal architecture design based on minimal surfaces: a compromise between permeability and elastic properties. Mater Des 126:98–114. https://doi.org/10.1016/j.matdes.2017.04.009
64. Callens SJP, Uyttendaele RJC, Fratila-Apachitei LE et al (2020) Substrate curvature as a cue to guide spatiotemporal cell and tissue organization. Biomaterials 232:119739. https://doi.org/10.1016/j.biomaterials.2019.119739
65. Prakoso AT, Basri H, Adanta D et al (2023) The effect of tortuosity on permeability of porous scaffold. Biomedicines 11(2): 427. https://doi.org/10.3390/biomedicines11020427
66. Blanquer SBG, Werner M, Hannula M et al (2017) Surface curvature in triply-periodic minimal surface architectures as a distinct design parameter in preparing advanced tissue engineering scaffolds. Biofabrication 9(2):025001. https://doi.org/10.1088/1758-5090/aa6553
67. Bobbert FL, Lietaert K, Eftekhari AA et al (2017) Additively manufactured metallic porous biomaterials based on minimal surfaces: a unique combination of topological, mechanical, and mass transport properties. Acta Biomater 53:572–584. https://doi.org/10.1016/j.actbio.2017.02.024
68. Zhang XY, Jiang L, Yan XC et al (2023) Revealing the apparent and local mechanical properties of heterogeneous lattice: a multi-scale study of functionally graded scaffold. Virt Phys Prototyp 18(1):e2120406. https://doi.org/10.1080/17452759.2022.2120406
69. Al-Ketan O, Lee DW, Rowshan R et al (2020) Functionally graded and multi-morphology sheet TPMS lattices: design, manufacturing, and mechanical properties. J Mech Behav Biomed Mater 102:103520. https://doi.org/10.1016/j.jmbbm.2019.103520
70. Shi JP, Zhu LY, Li L et al (2018) A TPMS-based method for modeling porous scaffolds for bionic bone tissue engineering. Sci Rep 8(1):7395. https://doi.org/10.1038/s41598-018-25750-9
71. Zhang XY, Yan XC, Fang G et al (2020) Biomechanical influence of structural variation strategies on functionally graded scaffolds constructed with triply periodic minimal surface. Addit Manuf 32:101015. https://doi.org/10.1016/j.addma.2019.101015
72. Torres Y, Trueba P, Pavón JJ et al (2016) Design, processing and characterization of titanium with radial graded porosity for bone implants. Mater Des 110:179–187. https://doi.org/10.1016/j.matdes.2016.07.135
73. Liu F, Mao ZF, Zhang P et al (2018) Functionally graded porous scaffolds in multiple patterns: new design method, physical and mechanical properties. Mater Des 160:849–860. https://doi.org/10.1016/j.matdes.2018.09.053
74. Wang S, Shi ZA, Liu LL et al (2020) The design of Ti6Al4V Primitive surface structure with symmetrical gradient of pore size in biomimetic bone scaffold. Mater Des 193:108830. https://doi.org/10.1016/j.matdes.2020.108830
75. Bora R, Shukla M, Kumar A (2023) Finite element analysis based design of biomimetic functionally graded Ti-6Al-4V alloy scaffolds for human cortical bone applications. Mater Today Proc 90:81–85. https://doi.org/10.1016/j.matpr.2023.05.057
76. Song CH, Chen JQ, Lei HY et al (2024) Radial gradient design enabling additively manufactured low-modulus gyroid tantalum structures. Int J Mech Sci 262:108710. https://doi.org/10.1016/j.ijmecsci.2023.108710
77. Zhang Q, Ma LM, Ji XF et al (2022) High-strength hydroxyapatite scaffolds with minimal surface macrostructures for load-bearing bone regeneration. Adv Funct Mater 32(33): 2204182. https://doi.org/10.1002/adfm.202204182
78. Davoodi E, Montazerian H, Esmaeilizadeh R et al (2021) Additively manufactured gradient porous Ti-6Al-4V hip replacement implants embedded with cell-laden gelatin methacryloyl hydrogels. ACS Appl Mater Interfaces 13(19):22110–22123. https://doi.org/10.1021/acsami.0c20751
79. Hu JB, Wang SF, Li BJ et al (2022) Efficient representation and optimization for TPMS-based porous structures. IEEE Trans Vis Comput Graph 28(7):2615–2627. https://doi.org/10.1109/TVCG.2020.3037697
80. Tripathi Y, Shukla M (2017) Triply periodic minimal surface based geometry design of bio-scaffolds. In: International Conference on Advances in Mechanical, Industrial, Automation and Management Systems, p.348–350. https://doi.org/10.1109/AMIAMS.2017.8069237
81. Ma SH, Song KL, Lan J et al (2020) Biological and mechanical property analysis for designed heterogeneous porous scaffolds based on the refined TPMS. J Mech Behav Biomed Mater 107: 103727. https://doi.org/10.1016/j.jmbbm.2020.103727
82. Ding JH, Zou Q, Qu S et al (2021) STL-free design and manufacturing paradigm for high-precision powder bed fusion. CIRP Ann 70(1):167–170. https://doi.org/10.1016/j.cirp.2021.03.012
83. Yoo DJ (2013) New paradigms in hierarchical porous scaffold design for tissue engineering. Mater Sci Eng C Mater Biol Appl 33(3):1759–1772. https://doi.org/10.1016/j.msec.2012.12.092
84. Zou SJ, Mu YR, Pan BC et al (2022) Mechanical and biological properties of enhanced porous scaffolds based on triply periodic minimal surfaces. Mater Des 219:110803. https://doi.org/10.1016/j.matdes.2022.110803
85. Feng JW, Fu JZ, Shang C et al (2020) Efficient generation strategy for hierarchical porous scaffolds with freeform external geometries. Addit Manuf 31:100943. https://doi.org/10.1016/j.addma.2019.100943
86. Li L, Wang P, Liang HX et al (2023) Design of a Haversian system-like gradient porous scaffold based on triply periodic minimal surfaces for promoting bone regeneration. J Adv Res 54:89–104. https://doi.org/10.1016/j.jare.2023.01.004
87. Luo WW, Wang Y, Wang ZH et al (2024) Advanced topology of triply periodic minimal surface structure for osteogenic improvement within orthopedic metallic screw. Mater Today Bio 27:101118. https://doi.org/10.1016/j.mtbio.2024.101118
88. Rezapourian M, Kamboj N, Jasiuk I et al (2022) Biomimetic design of implants for long bone critical-sized defects. J Mech Behav Biomed Mater 134:105370. https://doi.org/10.1016/j.jmbbm.2022.105370
89. Zhao M, Li XW, Zhang DZ et al (2023) TPMS-based interpenetrating lattice structures: design, mechanical properties and multiscale optimization. Int J Mech Sci 244:108092. https://doi.org/10.1016/j.ijmecsci.2022.108092
90. Khaleghi S, Dehnavi FN, Baghani M et al (2021) On the directional elastic modulus of the TPMS structures and a novel hybridization method to control anisotropy. Mater Des 210: 110074. https://doi.org/10.1016/j.matdes.2021.110074
91. Nazir A, Hussain S, Ali HM et al (2024) Design and mechanical performance of nature-inspired novel hybrid triply periodic minimal surface lattice structures fabricated using material extrusion. Mater Today Commun 38:108349. https://doi.org/10.1016/j.mtcomm.2024.108349

92. Chen ZY, Xie YM, Wu X et al (2019) On hybrid cellular materials based on triply periodic minimal surfaces with extreme mechanical properties. Mater Des 183:108109. https://doi.org/10.1016/j.matdes.2019.108109
93. Zhang XN, Yan SL, Xie XY et al (2024) Multi-dimensional hybridized TPMS with high energy absorption capacity. Int J Mech Sci 273:109244. https://doi.org/10.1016/j.ijmecsci.2024.109244
94. Gao TY, Liu K, Wang XX et al (2024) Multi-level mechanism of biomimetic TPMS hybridizations with tailorable global homogeneity and heterogeneity. Extreme Mech Lett 68:102136. https://doi.org/10.1016/j.eml.2024.102136
95. Li FL, Gan JK, Zhang L et al (2024) Enhancing impact resistance of hybrid structures designed with triply periodic minimal surfaces. Compos Sci Technol 245:110365. https://doi.org/10.1016/j.compscitech.2023.110365
96. Feng JW, Liu B, Lin ZW et al (2021) Isotropic porous structure design methods based on triply periodic minimal surfaces. Mater Des 210:110050. https://doi.org/10.1016/j.matdes.2021.110050
97. Figiel H, Żogał O, Yartys V (2005) Preface. J Alloys Compd 404–406:1. https://doi.org/10.1016/j.jallcom.2005.05.002
98. Alabort E, Barba D, Reed RC (2019) Design of metallic bone by additive manufacturing. Scr Mater 164:110–114. https://doi.org/10.1016/j.scriptamat.2019.01.022
99. Delgado-Ruiz R, Romanos G (2018) Potential causes of titanium particle and ion release in implant dentistry: a systematic review. Int J Mol Sci 19(11):E3585. https://doi.org/10.3390/ijms19113585
100. Sharma A, Oh MC, Kim JT et al (2020) Investigation of electrochemical corrosion behavior of additive manufactured Ti–6Al–4V alloy for medical implants in different electrolytes. J Alloys Compd 830:154620. https://doi.org/10.1016/j.jallcom.2020.154620
101. Koju N, Niraula S, Fotovvati B (2022) Additively manufactured porous Ti6Al4V for bone implants: a review. Metals 12(4):687. https://doi.org/10.3390/met12040687
102. Yan CZ, Hao L, Hussein A et al (2017) Microstructural and surface modifications and hydroxyapatite coating of Ti-6Al-4V triply periodic minimal surface lattices fabricated by selective laser melting. Mater Sci Eng C Mater Biol Appl 75:1515–1524. https://doi.org/10.1016/j.msec.2017.03.066
103. Xiong YZ, Han ZZ, Qin JW et al (2021) Effects of porosity gradient pattern on mechanical performance of additive manufactured Ti-6Al-4V functionally graded porous structure. Mater Des 208:109911. https://doi.org/10.1016/j.matdes.2021.109911
104. Yan C, Hao L, Hussein A et al (2015) Ti-6Al-4V triply periodic minimal surface structures for bone implants fabricated via selective laser melting. J Mech Behav Biomed Mater 51:61–73. https://doi.org/10.1016/j.jmbbm.2015.06.024
105. Ataee A, Li YC, Fraser D et al (2018) Anisotropic Ti-6Al-4V gyroid scaffolds manufactured by electron beam melting (EBM) for bone implant applications. Mater Des 137:345–354. https://doi.org/10.1016/j.matdes.2017.10.040
106. Tilton M, Borjali A, Griffis JC et al (2023) Fatigue properties of Ti-6Al-4V TPMS scaffolds fabricated via laser powder bed fusion. Manuf Lett 37:32–38. https://doi.org/10.1016/j.mfglet.2023.06.005
107. Rezapourian M, Jasiuk I, Saarna M et al (2023) Selective laser melted Ti6Al4V split-P TPMS lattices for bone tissue engineering. Int J Mech Sci 251:108353. https://doi.org/10.1016/j.ijmecsci.2023.108353
108. Corona-Castuera J, Rodriguez-Delgado D, Henao J et al (2021) Design and fabrication of a customized partial hip prosthesis employing CT-scan data and lattice porous structures. ACS Omega 6(10):6902–6913. https://doi.org/10.1021/acsomega.0c06144
109. Ravichander BB, Jagdale SH, Jabed A et al (2023) Mechanical and corrosion behavior of sheet-based 316L TPMS structures. Int J Mech Sci 254:108439. https://doi.org/10.1016/j.ijmecsci.2023.108439
110. Luo ZC, Tang Q, Feng QX et al (2023) Finite element analysis on mechanical properties of selective laser melting-produced stainless steel 316L lattice structures under impact loading. J Mater Eng Perform 32(1):438–449. https://doi.org/10.1007/s11665-022-07104-9
111. Wang NY, Meenashisundaram GK, Chang S et al (2022) A comparative investigation on the mechanical properties and cytotoxicity of Cubic, Octet, and TPMS gyroid structures fabricated by selective laser melting of stainless steel 316L. J Mech Behav Biomed Mater 129:105151. https://doi.org/10.1016/j.jmbbm.2022.105151
112. Szatkiewicz T, Laskowska D, Bałasz B et al (2022) The influence of the structure parameters on the mechanical properties of cylindrically mapped gyroid TPMS fabricated by selective laser melting with 316L stainless steel powder. Materials 15(12):4352. https://doi.org/10.3390/ma15124352
113. Ma S, Tang Q, Feng QX et al (2019) Mechanical behaviours and mass transport properties of bone-mimicking scaffolds consisted of gyroid structures manufactured using selective laser melting. J Mech Behav Biomed Mater 93:158–169. https://doi.org/10.1016/j.jmbbm.2019.01.023
114. Gatto ML, Cerqueni G, Groppo R et al (2023) Improved biomechanical behavior of 316L graded scaffolds for bone tissue regeneration produced by laser powder bed fusion. J Mech Behav Biomed Mater 144:105989. https://doi.org/10.1016/j.jmbbm.2023.105989
115. Cui YL, Gain AK, Zhang LC et al (2024) Manufacture and property characterization of interconnected pore-gradient TPMS materials. Mater Sci Eng A 892:146100. https://doi.org/10.1016/j.msea.2024.146100
116. Foroughi AH, Liu DH, Razavi MJ (2023) Simultaneous optimization of stiffness, permeability, and surface area in metallic bone scaffolds. Int J Eng Sci 193:103961. https://doi.org/10.1016/j.ijengsci.2023.103961
117. Zhu JJ, Zou SJ, Mu YR et al (2022) Additively manufactured scaffolds with optimized thickness based on triply periodic minimal surface. Materials 15(20):7084. https://doi.org/10.3390/ma15207084
118. Yang L, Yan CZ, Cao WC et al (2019) Compression–compression fatigue behaviour of gyroid-type triply periodic minimal surface porous structures fabricated by selective laser melting. Acta Mater 181:49–66. https://doi.org/10.1016/j.actamat.2019.09.042
119. Karunakaran R, Ortgies S, Tamayol A et al (2020) Additive manufacturing of magnesium alloys. Bioact Mater 5(1):44–54. https://doi.org/10.1016/j.bioactmat.2019.12.004
120. Zeng ZR, Salehi M, Kopp A et al (2022) Recent progress and perspectives in additive manufacturing of magnesium alloys. J Magnes Alloys 10(6):1511–1541. https://doi.org/10.1016/j.jma.2022.03.001
121. Kaushik V, Kumar BN, Kumar SS et al (2022) Magnesium role in additive manufacturing of biomedical implants–challenges and opportunities. Addit Manuf 55:102802. https://doi.org/10.1016/j.addma.2022.102802
122. Allavikutty R, Gupta P, Santra TS et al (2021) Additive manufacturing of Mg alloys for biomedical applications: current status and challenges. Curr Opin Biomed Eng 18:100276.

https://doi.org/10.1016/j.cobme.2021.100276
123. Peng B, Xu HJ, Song F et al (2024) Additive manufacturing of porous magnesium alloys for biodegradable orthopedic implants: process, design, and modification. J Mater Sci Technol 182:79–110. https://doi.org/10.1016/j.jmst.2023.08.072
124. Temiz A, Yaşar M, Koç E (2022) Fabrication of open-pore biodegradable magnesium alloy scaffold via infiltration technique. Int J Met 16(1):317–328. https://doi.org/10.1007/s40962-021-00604-9
125. Ren JH, Xia ZW, Chen BX et al (2024) Development of biodegradable Zn-based porous scaffolds with elaborate triply periodic minimal surface structure via Vat photopolymerization-assisted template replacement strategy. J Mater Res Technol 30:6050–6063. https://doi.org/10.1016/j.jmrt.2024.05.035
126. Yin BZ, Liu JG, Peng B et al (2024) Influence of layer thickness on formation quality, microstructure, mechanical properties, and corrosion resistance of WE43 magnesium alloy fabricated by laser powder bed fusion. J Magnes Alloys 12(4):1367–1385. https://doi.org/10.1016/j.jma.2022.09.016
127. Wang CX, Liu JG, Min SY et al (2023) The effect of pore size on the mechanical properties, biodegradation and osteogenic effects of additively manufactured magnesium scaffolds after high temperature oxidation: an in vitro and in vivo study. Bioact Mater 28:537–548. https://doi.org/10.1016/j.bioactmat.2023.06.009
128. Liu JG, Liu BC, Min SY et al (2022) Biodegradable magnesium alloy WE43 porous scaffolds fabricated by laser powder bed fusion for orthopedic applications: process optimization, in vitro and in vivo investigation. Bioact Mater 16:301–319. https://doi.org/10.1016/j.bioactmat.2022.02.020
129. Yue XZ, Shang JT, Zhang MH et al (2022) Additive manufacturing of high porosity magnesium scaffolds with lattice structure and random structure. Mater Sci Eng A 859:144167. https://doi.org/10.1016/j.msea.2022.144167
130. Kapanen A, Ryhänen J, Danilov A et al (2001) Effect of nickel-titanium shape memory metal alloy on bone formation. Biomaterials 22(18):2475–2480. https://doi.org/10.1016/s0142-9612(00)00435-x
131. Kujala S, Ryhänen J, Danilov A et al (2003) Effect of porosity on the osteointegration and bone ingrowth of a weight-bearing nickel-titanium bone graft substitute. Biomaterials 24(25):4691–4697. https://doi.org/10.1016/s0142-9612(03)00359-4
132. Yang X, Yang Q, Shi YS et al (2022) Effect of volume fraction and unit cell size on manufacturability and compressive behaviors of Ni-Ti triply periodic minimal surface lattices. Addit Manuf 54:102737. https://doi.org/10.1016/j.addma.2022.102737
133. Speirs M, Van Hooreweder B, Van Humbeeck J et al (2017) Fatigue behaviour of NiTi shape memory alloy scaffolds produced by SLM, a unit cell design comparison. J Mech Behav Biomed Mater 70:53–59. https://doi.org/10.1016/j.jmbbm.2017.01.016
134. Shiva S, Palani IA, Mishra SK et al (2015) Investigations on the influence of composition in the development of Ni–Ti shape memory alloy using laser based additive manufacturing. Opt Laser Technol 69:44–51. https://doi.org/10.1016/j.optlastec.2014.12.014
135. Mahmoudi M, Tapia G, Franco B et al (2018) On the printability and transformation behavior of nickel-titanium shape memory alloys fabricated using laser powder-bed fusion additive manufacturing. J Manuf Process 35:672–680. https://doi.org/10.1016/j.jmapro.2018.08.037
136. Lv YT, Liu GH, Wang BH et al (2022) Pore strategy design of a novel NiTi-Nb biomedical porous scaffold based on a triply periodic minimal surface. Front Bioeng Biotechnol 10:910475. https://doi.org/10.3389/fbioe.2022.910475
137. Sun LQ, Chen KY, Geng P et al (2023) Mechanical and shape memory properties of NiTi triply periodic minimal surface structures fabricated by laser powder bed fusion. J Manuf Process 101:1091–1100. https://doi.org/10.1016/j.jmapro.2023.06.034
138. Hussain S, Alagha AN, Haidemenopoulos GN et al (2023) Microstructural and surface analysis of NiTi TPMS lattice sections fabricated by laser powder bed fusion. J Manuf Process 102:375–386. https://doi.org/10.1016/j.jmapro.2023.07.055
139. Hussain S, Alagha AN, Zaki W (2025) Phase transformation behavior of NiTi triply periodic minimal surface lattices fabricated by laser powder bed fusion. J Mater Eng Perform 34(2):1136–1148. https://doi.org/10.1007/s11665-024-09162-7
140. Hussain S, Alagha AN, Zaki W (2022) Imperfections formation in thin layers of NiTi triply periodic minimal surface lattices fabricated using laser powder bed fusion. Materials 15(22):7950. https://doi.org/10.3390/ma15227950
141. Zhang C, Jin JL, He M et al (2022) Compressive mechanics and hyperelasticity of Ni-Ti lattice structures fabricated by selective laser melting. Crystals 12(3):408. https://doi.org/10.3390/cryst12030408
142. Tang DY, Hu Y, Yang L (2023) New insights into the mechanical properties, functional fatigue, and structural fatigue of Ni-Ti alloy porous structures. Metals 13(5):931. https://doi.org/10.3390/met13050931
143. Jin JL, Wu SQ, Yang L et al (2024) Ni–Ti multicell interlacing Gyroid lattice structures with ultra-high hyperelastic response fabricated by laser powder bed fusion. Int J Mach Tools Manuf 195:104099. https://doi.org/10.1016/j.ijmachtools.2023.104099
144. Zhang YT, Wang LQ, Lan CG et al (2024) Microstructure-dependent deformation mechanisms and fracture modes of gradient porous NiTi alloys. Mater Des 243:113049. https://doi.org/10.1016/j.matdes.2024.113049
145. Chen WL, Yang JZ, Kong H et al (2021) Fatigue behaviour and biocompatibility of additively manufactured bioactive tantalum graded lattice structures for load-bearing orthopaedic applications. Mater Sci Eng C Mater Biol Appl 130:112461. https://doi.org/10.1016/j.msec.2021.112461
146. Han Q, Wang CY, Chen H et al (2019) Porous tantalum and titanium in orthopedics: a review. ACS Biomater Sci Eng 5(11):5798–5824. https://doi.org/10.1021/acsbiomaterials.9b00493
147. Soro N, Brodie EG, Abdal-hay A et al (2022) Additive manufacturing of biomimetic titanium-tantalum lattices for biomedical implant applications. Mater Des 218:110688. https://doi.org/10.1016/j.matdes.2022.110688
148. Liu YD, Bao CY, Wismeijer D et al (2015) The physicochemical/biological properties of porous tantalum and the potential surface modification techniques to improve its clinical application in dental implantology. Mater Sci Eng C Mater Biol Appl 49:323–329. https://doi.org/10.1016/j.msec.2015.01.007
149. Lu T, Wen J, Qian S et al (2015) Enhanced osteointegration on tantalum-implanted polyetheretherketone surface with bone-like elastic modulus. Biomaterials 51:173–183. https://doi.org/10.1016/j.biomaterials.2015.02.018
150. Zhang YT, Aiyiti W, Du S et al (2023) Design and mechanical behaviours of a novel tantalum lattice structure fabricated by

SLM. Virt Phys Prototyp 18(1):e2192702. https://doi.org/10.1080/17452759.2023.2192702
151. Wauthle R, van der Stok J, Amin Yavari S et al (2015) Additively manufactured porous tantalum implants. Acta Biomater 14:217–225. https://doi.org/10.1016/j.actbio.2014.12.003
152. Chen JQ, Song CH, Deng ZT et al (2024) Functional gradient design of additive manufactured gyroid tantalum porous structures: manufacturing, mechanical behaviors and permeability. J Manuf Process 125:202–216. https://doi.org/10.1016/j.jmapro.2024.07.054
153. Wei S, Xu CT, Zhang RG et al (2024) Fabrication and characterization of porous Ta/CHS/n-HA composite scaffolds based on SLM technology. https://doi.org/10.21203/rs.3.rs-3825380/v1
154. Shekhawat D, Singh A, Bhardwaj A et al (2021) A short review on polymer, metal and ceramic based implant materials. IOP Conf Ser Mater Sci Eng 1017(1):012038. https://doi.org/10.1088/1757-899x/1017/1/012038
155. Maskery I, Sturm L, Aremu AO et al (2018) Insights into the mechanical properties of several triply periodic minimal surface lattice structures made by polymer additive manufacturing. Polymer 152:62–71. https://doi.org/10.1016/j.polymer.2017.11.049
156. Abueidda DW, Bakir M, Abu Al-Rub RK et al (2017) Mechanical properties of 3D printed polymeric cellular materials with triply periodic minimal surface architectures. Mater Des 122:255–267. https://doi.org/10.1016/j.matdes.2017.03.018
157. Park SI, Rosen DW, Choi SK et al (2014) Effective mechanical properties of lattice material fabricated by material extrusion additive manufacturing. Addit Manuf 1–4:12–23. https://doi.org/10.1016/j.addma.2014.07.002
158. Ozbolat IT, Hospodiuk M (2016) Current advances and future perspectives in extrusion-based bioprinting. Biomaterials 76: 321–343. https://doi.org/10.1016/j.biomaterials.2015.10.076
159. Noroozi R, Tatar F, Zolfagharian A et al (2022) Additively manufactured multi-morphology bone-like porous scaffolds: experiments and micro-computed tomography-based finite element modeling approaches. Int J Bioprint 8(3):556. https://doi.org/10.18063/ijb.v8i3.556
160. Hoque ME, Chuan YL, Pashby I (2012) Extrusion based rapid prototyping technique: an advanced platform for tissue engineering scaffold fabrication. Biopolymers 97(2):83–93. https://doi.org/10.1002/bip.21701
161. Diez-Escudero A, Harlin H, Isaksson P et al (2020) Porous polylactic acid scaffolds for bone regeneration: a study of additively manufactured triply periodic minimal surfaces and their osteogenic potential. J Tissue Eng 11:2041731420956541. https://doi.org/10.1177/2041731420956541
162. Al Hashimi NS, Soman SS, Govindharaj M et al (2022) 3D printing of complex architected metamaterial structures by simple material extrusion for bone tissue engineering. Mater Today Commun 31:103382. https://doi.org/10.1016/j.mtcomm.2022.103382
163. Sabahi N, Farajzadeh E, Roohani I et al (2024) Material extrusion 3D printing of polyether-ether-ketone scaffolds based on triply periodic minimal surface designs: a numerical and experimental investigation. Appl Mater Today 39:102262. https://doi.org/10.1016/j.apmt.2024.102262
164. Du XY, Ronayne S, Lee SS et al (2023) 3D-printed PEEK/silicon nitride scaffolds with a triply periodic minimal surface structure for spinal fusion implants. ACS Appl Bio Mater 6(8):3319–3329. https://doi.org/10.1021/acsabm.3c00383
165. Tripathi Y, Shukla M, Bhatt AD (2019) Implicit-function-based design and additive manufacturing of triply periodic minimal surfaces scaffolds for bone tissue engineering. J Mater Eng Perform 28(12):7445–7451. https://doi.org/10.1007/s11665-019-04457-6
166. Oladapo BI, Kayode JF, Karagiannidis P et al (2022) Polymeric composites of cubic-octahedron and gyroid lattice for biomimetic dental implants. Mater Chem Phys 289:126454. https://doi.org/10.1016/j.matchemphys.2022.126454
167. Oladapo B, Zahedi A, Ismail S et al (2023) 3D-printed biomimetic bone implant polymeric composite scaffolds. Int J Adv Manuf Technol 126(9):4259–4267. https://doi.org/10.1007/s00170-023-11344-x
168. Alkebsi EAA, Outtas T, Almutawakel A et al (2023) Design of mechanically compatible lattice structures cancellous bone fabricated by fused filament fabrication of Z-ABS material. Mech Adv Mater Struct 30(11):2269–2283. https://doi.org/10.1080/15376494.2022.2053904
169. Guo W, Yang YJ, Liu C et al (2023) 3D printed TPMS structural PLA/GO scaffold: process parameter optimization, porous structure, mechanical and biological properties. J Mech Behav Biomed Mater 142:105848. https://doi.org/10.1016/j.jmbbm.2023.105848
170. Agarwal R, Malhotra S, Gupta V et al (2023) Three-dimensional printing of triply periodic minimal surface structured scaffolds for load-bearing bone defects. Polym Eng Sci 63(3):972–985. https://doi.org/10.1002/pen.26258
171. Wang HZ, Chen P, Wu HZ et al (2022) Comparative evaluation of printability and compression properties of poly-ether-ether-ketone triply periodic minimal surface scaffolds fabricated by laser powder bed fusion. Addit Manuf 57:102961. https://doi.org/10.1016/j.addma.2022.102961
172. Sala R, Regondi S, Graziosi S et al (2022) Insights into the printing parameters and characterization of thermoplastic polyurethane soft triply periodic minimal surface and honeycomb lattices for broadening material extrusion applicability. Addit Manuf 58:102976. https://doi.org/10.1016/j.addma.2022.102976
173. Lumba LT, Chernyshikhin S, Mahato B et al (2023) The assessment of permeability of biological implant structure using DLP-manufactured TPMS lattice physical models. Mater Today Proc (early access). https://doi.org/10.1016/j.matpr.2023.10.092
174. Gabrieli R, Wenger R, Mazza M et al (2024) Design, stereolithographic 3D printing, and characterization of TPMS scaffolds. Materials 17(3):654. https://doi.org/10.3390/ma17030654
175. Budharaju H, Suresh S, Sekar MP et al (2023) Ceramic materials for 3D printing of biomimetic bone scaffolds–current state-of-the-art & future perspectives. Mater Des 231:112064. https://doi.org/10.1016/j.matdes.2023.112064.
176. Romanczuk-Ruszuk E, Sztorch B, Pakuła D et al (2023) 3D printing ceramics: materials for direct extrusion process. Ceramics 6(1):364–385. https://doi.org/10.3390/ceramics6010022
177. Trombetta R, Inzana JA, Schwarz EM et al (2017) 3D printing of calcium phosphate ceramics for bone tissue engineering and drug delivery. Ann Biomed Eng 45(1):23–44. https://doi.org/10.1007/s10439-016-1678-3
178. Zhong GY, Vaezi M, Liu P et al (2017) Characterization approach on the extrusion process of bioceramics for the 3D printing of bone tissue engineering scaffolds. Ceram Int 43(16): 13860–13868. https://doi.org/10.1016/j.ceramint.2017.07.109
179. Ang X, Tey JY, Yeo WH et al (2023) A review on metallic and

ceramic material extrusion method: materials, rheology, and printing parameters. J Manuf Process 90:28–42. https://doi.org/10.1016/j.jmapro.2023.01.077
180. Baumer V, Gunn E, Riegle V et al (2023) Robocasting of ceramic Fischer–Koch S scaffolds for bone tissue engineering. J Funct Biomater 14(5):251. https://doi.org/10.3390/jfb14050251
181. Restrepo S, Ocampo S, Ramírez JA et al (2017) Mechanical properties of ceramic structures based on triply periodic minimal surface (TPMS) processed by 3D printing. J Phys Conf Ser 935: 012036. https://doi.org/10.1088/1742-6596/935/1/012036
182. Charbonnier B, Manassero M, Bourguignon M et al (2020) Custom-made macroporous bioceramic implants based on triply-periodic minimal surfaces for bone defects in load-bearing sites. Acta Biomater 109:254–266. https://doi.org/10.1016/j.actbio.2020.03.016
183. Kong DK, Guo AF, Wu HL et al (2023) Method for preparing biomimetic ceramic structures with high strength and high toughness. Ceram Int 49(24):40284–40296. https://doi.org/10.1016/j.ceramint.2023.10.001
184. Zhang YH, Zhang Q, He FP et al (2022) Fabrication of cancellous-bone-mimicking β-tricalcium phosphate bioceramic scaffolds with tunable architecture and mechanical strength by stereolithography 3D printing. J Eur Ceram Soc 42(14):6713–6720. https://doi.org/10.1016/j.jeurceramsoc.2022.07.033
185. Maevskaia E, Khera N, Ghayor C et al (2023) Three-dimensional printed hydroxyapatite bone substitutes designed by a novel periodic minimal surface algorithm are highly osteoconductive. 3D Print Addit Manuf 10(5):905–916. https://doi.org/10.1089/3dp.2022.0134
186. Bouakaz I, Drouet C, Grossin D et al (2023) Hydroxyapatite 3D-printed scaffolds with Gyroid-triply periodic minimal surface porous structure: fabrication and an in vivo pilot study in sheep. Acta Biomater 170:580–595. https://doi.org/10.1016/j.actbio.2023.08.041
187. Maevskaia E, Ghayor C, Bhattacharya I et al (2024) TPMS microarchitectures for vertical bone augmentation and osteoconduction: an in vivo study. Materials 17(11):2533. https://doi.org/10.3390/ma17112533
188. Liang HW, Wang Y, Chen SS et al (2022) Nano-hydroxyapatite bone scaffolds with different porous structures processed by digital light processing 3D printing. Int J Bioprint 8(1):502. https://doi.org/10.18063/ijb.v8i1.502
189. Yao YX, Qin W, Xing BH et al (2021) High performance hydroxyapatite ceramics and a triply periodic minimum surface structure fabricated by digital light processing 3D printing. J Adv Ceram 10(1):39–48. https://doi.org/10.1007/s40145-020-0415-4
190. Hua SB, Yuan X, Wu JM et al (2022) Digital light processing porous TPMS structural HA & akermanite bioceramics with optimized performance for cancellous bone repair. Ceram Int 48(3):3020–3029. https://doi.org/10.1016/j.ceramint.2021.10.003
191. Zhu H, Wang JS, Wang SF et al (2024) Additively manufactured bioceramic scaffolds based on triply periodic minimal surfaces for bone regeneration. J Tissue Eng 15:20417314241244997. https://doi.org/10.1177/20417314241244997
192. Lu JX, Dong P, Zhao YT et al (2021) 3D printing of TPMS structural ZnO ceramics with good mechanical properties. Ceram Int 47(9):12897–12905. https://doi.org/10.1016/j.ceramint.2021.01.152
193. Jiao C, Xie DQ, He ZJ et al (2022) Additive manufacturing of bio-inspired ceramic bone scaffolds: structural design, mechanical properties and biocompatibility. Mater Des 217:110610. https://doi.org/10.1016/j.matdes.2022.110610
194. Shao HF, Zhu JH, Zhao X et al (2024) Additive manufacturing of magnesium-doped calcium silicate/zirconia ceramic scaffolds with projection-based 3D printing: sintering, mechanical and biological behavior. Ceram Int 50(6):9280–9292. https://doi.org/10.1016/j.ceramint.2023.12.244
195. Shen MD, Li YF, Lu FL et al (2023) Bioceramic scaffolds with triply periodic minimal surface architectures guide early-stage bone regeneration. Bioact Mater 25:374–386. https://doi.org/10.1016/j.bioactmat.2023.02.012
196. Duque-Uribe C, López-Vargas V, Moreno-Florez AI et al (2024) Production of ceramic alumina scaffolds via ceramic stereolithography with potential application in bone tissue regeneration. Mater Today Commun 40:109535. https://doi.org/10.1016/j.mtcomm.2024.109535
197. Li YF, Li JF, Jiang S et al (2023) The design of strut/TPMS-based pore geometries in bioceramic scaffolds guiding osteogenesis and angiogenesis in bone regeneration. Mater Today Bio 20: 100667. https://doi.org/10.1016/j.mtbio.2023.100667
198. Vijayavenkataraman S, Kuan LY, Lu WF (2020) 3D-printed ceramic triply periodic minimal surface structures for design of functionally graded bone implants. Mater Des 191:108602. https://doi.org/10.1016/j.matdes.2020.108602
199. Cao ET, Dong ZC, Zhang XJ et al (2023) Mechanical properties and failure analysis of 3D-printing micron-scale ceramic-based triply periodic minimal surface scaffolds under quasi-static-compression and low-speed impact loads. Compos Sci Technol 243:110248. https://doi.org/10.1016/j.compscitech.2023.110248
200. Xu Y, Zhang SJ, Ding WH et al (2024) Additively-manufactured gradient porous bio-scaffolds: permeability, cytocompatibility and mechanical properties. Compos Struct 336: 118021. https://doi.org/10.1016/j.compstruct.2024.118021
201. Viet NV, Waheed W, Alazzam A et al (2023) Effective compressive behavior of functionally graded TPMS titanium implants with ingrown cortical or trabecular bone. Compos Struct 303:116288. https://doi.org/10.1016/j.compstruct.2022.116288
202. Zhianmanesh M, Varmazyar M, Montazerian H (2019) Fluid permeability of graded porosity scaffolds architectured with minimal surfaces. ACS Biomater Sci Eng 5(3):1228–1237. https://doi.org/10.1021/acsbiomaterials.8b01400
203. Zhang ZY, Zhang H, Zhang J et al (2023) Study on flow field characteristics of TPMS porous materials. J Braz Soc Mech Sci Eng 45(4):188. https://doi.org/10.1007/s40430-023-04113-0
204. Liu ZQ, Gong H, Gao JZ et al (2023) Bio-inspired design, mechanical and mass-transport characterizations of orthotropic TPMS-based scaffold. Compos Struct 321:117256. https://doi.org/10.1016/j.compstruct.2023.117256
205. Zhou J, Gui YQ, Xu QP et al (2024) Investigation of permeability and biocompatibility of TPMS structures printed by laser powder bed fusion using Ti64-5Cu alloy for orthopedic implants. Mater Lett 355:135552. https://doi.org/10.1016/j.matlet.2023.135552
206. Castro APG, Santos J, Pires T et al (2020) Micromechanical behavior of TPMS scaffolds for bone tissue engineering. Macromol Mater Eng 305(12):2000487. https://doi.org/10.1002/mame.202000487
207. Karaman D, Asl HG (2023) The effects of sheet and network solid structures of similar TPMS scaffold architectures on permeability, wall shear stress, and velocity: a CFD analysis.

Med Eng Phys 118:104024.
https://doi.org/10.1016/j.medengphy.2023.104024
208. Pires T, Santos J, Ruben RB et al (2021) Numerical-experimental analysis of the permeability-porosity relationship in triply periodic minimal surfaces scaffolds. J Biomech 117: 110263.
https://doi.org/10.1016/j.jbiomech.2021.110263
209. Maevskaia E, Guerrero J, Ghayor C et al (2023) Triply periodic minimal surface-based scaffolds for bone tissue engineering: a mechanical, in vitro and in vivo study. Tissue Eng Part A 29(19–20):507–517.
https://doi.org/10.1089/ten.TEA.2023.0033
210. Li L, Shi JP, Zhang KJ et al (2019) Early osteointegration evaluation of porous Ti6Al4V scaffolds designed based on triply periodic minimal surface models. J Orthop Translat 19:94–105.
https://doi.org/10.1016/j.jot.2019.03.003
211. Khan PA, Raheem A, Kalirajan C et al (2024) In vivo assessment of a triple periodic minimal surface based biomimmetic gyroid as an implant material in a rabbit tibia model. ACS Mater Au 4(5):479–488.
https://doi.org/10.1021/acsmaterialsau.4c00016
212. Wang X, Liu AB, Zhang ZB et al (2024) Additively manufactured Zn-2Mg alloy porous scaffolds with customizable biodegradable performance and enhanced osteogenic ability. Adv Sci 11(5):e2307329.
https://doi.org/10.1002/advs.202307329